Inferring the environmental conditions present during early tetrapod terrestrialization from skeletal $\delta^{18}O$ values

---

A Thesis presented to the Faculty of the Graduate School at the University of Missouri-Columbia

---

In Partial Fulfillment of the Requirements for the Degree Master of Science

---

by

Rachael Savoie

Dr. Kenneth G. MacLeod, Thesis Supervisor

MAY 2023

The undersigned, appointed by the dean of the Graduate School, have examined the thesis entitled

Inferring the environmental conditions present during early tetrapod terrestrialization from skeletal δ18O values

presented by Rachael Savoie,

a candidate for the degree of Master of Science,

and hereby certify that, in their opinion, it is worthy of acceptance.

Professor Kenneth MacLeod

Professor Sarah Jacquet

Professor James Schiffbauer

Acknowledgments

I would like to thank my advisor, Ken MacLeod, for accepting me as his student and allowing me to continue and expand upon research I began in my undergraduate studies for my Master's thesis. Thank you for your patience, your enthusiasm, and for always pushing me to strive for success.

I would also like to thank my committee members, Jim Schiffbauer and Sarah Jacquet for their support and feedback. Viorel Atudorei was a tremendous help in the analyses of the samples used in this study, and I thank him for his extensive help, knowledge, and enthusiasm. Thank you to the Department of Geological Sciences for providing the financial support which made this research possible.

This project would not have been possible without the generous donation of fossil material from Ted Daeschler, and the help and support from my undergraduate advisors Page Quinton and Michael Rygel who took me in as a young researcher.

Lastly, I would like to thank my partner Aidan and my parents for being there for me while I work to achieve my dreams.

Table of Contents

List of figures……..vi

List of tables……...…….vi

Abstract……..……vii

1 Introduction……...……...…1

2 Background: Red Hill, Pennsylvania……..….8

3 Background: Joggins Fossil Cliffs, Nova Scotia……..…….12

4 Background: Technical History…….16

4.1 Palaeothermometry …….....16

4.2 Fractionation Processes……..17

4.3 History of techniques used for isotopic analysis……18

5 Materials and Methods……...20

5.1 Sample preparation……20

5.1.1 Red Hill……..20

5.1.2 The Joggins Formation……..22

5.2 Analytical procedure……..25

5.2.1 Isolating the PO4 anion……..25

5.2.2 Mass spectrometry…….26

5.3 Data Correction……..26

5.4 $\delta^{18}O_{water}$ Estimates……..27

5.5 Red Hill floodplain faunal groups……..28

5.6 Marine model…….28

6 Results……30

6.1 Red Hill, Pennsylvania ….…….30

6.1.1 Variability in $\delta^{18}O_{water}$ across the floodplain……..30

6.1.2 Variability within individuals and sample types ……...…31

6.2 The Joggins Formation, Nova Scotia…….35

6.2.1 Oxygen isotopic value of water through the section……..35

6.2.2 Calculated marine contribution……..36

7 Discussion……..…38
7.1 Red Hill, Pennsylvania ……..…38
7.1.1 Possible explanations for the lack of evidence for evaporation….38
7.1.2 Variability within organisms and sample types ……40
7.2 The Joggins Formation, Nova Scotia……..…42
7.3 Freshwater dominance during the deposition of the Joggins Formation...42
8 Conclusions……47
Bibliography……..…56

List of Figures:

Figure 1: Devonian and Carboniferous time scale and time rock scale.....6
Figure 2: Map of the modern and ancient location of the Joggins Formation and Red Hill site……...….7
Figure 3: Floodplain habitat reconstruction with associated average $\delta^{18}O_{water}$ values…11
Figure 4: Fossil material analyzed from Red Hill fauna……..….21
Figure 5: Stratigraphic column of the Joggins Formation from Grey et al. (2011) and sampled stratigraphic units……24
Figure 6: Plot of $\delta^{18}O_{phosphate}$ from organisms from the Red Hill floodplain……..….33
Figure 7: Plot of $\delta^{18}O_{phosphate}$ values over the cross section of tetrapodamorph teeth and scales……..…34
Figure 8: Average $\delta^{18}O_{water}$ of each stratigraphic unit ……37

List of Tables:

Table 1: Red Hill, Pennsylvania $\delta^{18}O$ data collected from analyses……..…50
Table 1: The Joggins Formation, Nova Scotia $\delta^{18}O$ data collected from analyses……..…53

Inferring the environmental conditions present during early tetrapod terrestrialization from skeletal $\delta^{18}O$ values

Rachael Savoie

Dr. Kenneth MacLeod, Thesis Supervisor

ABSTRACT

To test the extent of marine influence in the Joggins Formation, Nova Scotia, Canada and the possible habitat segregation and the net moisture balance at the Red Hill roadcut exposure of the Duncannon Member of the Catskill Formation in Pennsylvania, phosphatic fossils from both locations were analyzed to determine local and/ or regional changes in the oxygen isotopic composition of local surface waters. Marine to brackish taxa are present within the Joggins Formation, but disagreement exists over the degree of marine influence during deposition. In this study, the $\delta^{18}O_{water}$ values calculated for sections of the Joggins Formation compared with typical values for Carboniferous marine water don't reflect fully marine conditions but are consistent with a brackish setting in which seawater mixed with freshwater in the Cumberland Basin during the deposition of the Joggins Formation. Evidence of net evaporative conditions present in the sedimentological and paleontological record at the Red Hill floodplain suggest $\delta^{18}O$ of water would be high and variable. Variability in $\delta^{18}O$ across the floodplain show no general trends toward net evaporative conditions. However, variability within individuals does reflect variation in aquatic conditions, not artifacts related to sample types. Observations presented in this study provide independent constrains on two windows into the transition from fish to fully terrestrial vertebrates.

Introduction

The evolutionary history of organisms is strongly intertwined with the environments in which they lived. For the history of vertebrates, and thus us, the evolution of amphibious tetrapodamorphs is one of the most important evolutionary adaptations. The evolution of the tetrapod body plan laid the morphological and behavioral foundation for the major diversification of amphibians, reptiles, mammals, and birds. Vertebrate fossils documenting both the transition to four-legged locomotion and the appearance of the first reptiles which laid eggs on land are consistently found in floodplain environments (Carroll, 1964).

Describing the morphological changes that occurred during the evolution of walking limbs in vertebrates requires a good fossil record and the aggrading floodplain settings provide taphonomic conditions that promote a good fossil record. However, determining the details of the environment as it relates to possible selection pressures on the ancestors of reptiles requires integrated sedimentological, paleontological, and geochemical observations. This study uses $\delta^{18}O$ values preserved in fish and tetrapodamorph fossils to better constrain the environmental conditions in which terrestrial lifestyles evolved among vertebrates.

Evolution of tetrapods

During the Devonian (416 to 359 Ma) (Figure 1) the lobe-finned fishes were a diverse and successful group whose ecology and morphology would give some lineages a literal leg up on their contemporaries and open a path to the colonization of terrestrial environments. The first tetrapods emerged during the Frasnian Age (around 375-385

Ma), in the aquatic environments of modern Latvia and western Russia (Clack, 2002). By the Famennian, amphibious tetrapods existed alongside lobe-finned fish and transitionary species of tetrapods. From the end of the Frasnian to the early Carboniferous (375 to 223 Ma) tetrapods diversified and became widespread, and by the late Bashkirian age, the earliest amniotic (egg-laying) reptiles appeared, marking the first fully terrestrial vertebrates (Carroll, 1964; George and Blieck, 2011).

The tetrapodamorph clade includes crown group tetrapods, as well as stem group tetrapods which include taxa closely related to and descended from lobe-finned fish. Included in the clade is (1) the order osteolepiform lobe-finned fish, (2) the transitional order elipstostegalia taxa sometimes characterized as “fishapods” (a term coined by Neil Shubin (Shubin, 2006) with the discovery of *Tiktaalik*), and (3) early amphibious tetrapods placed in the order icthostegalia (Blieck et. al, 2007; Clack, 2002; Cloutier and Clement, 2020; Simoes et al. 2021). Generally, the evolution of the members of the tetrapodamorph clade is characterized by (1) the flattening and elongation of the head, (2) the skeletal morphology of the limbs, (3) and the adaptation to amphibious lifestyle (Clack, 2002; Simoes, 2021). Temnospondyls represent the transition from tetrapodamorph to tetrapod and are generally considered to be in the crown group Tetrapoda (Godfrey et al. 1987). Unlike the tetrapodamorphs, temnospondyls were predominantly terrestrial, returning to water only to mate, although some forms continued to live aquatic lifestyles despite their ability to walk on land (Clack, 2002).

Theories concerning selection favoring tetrapod evolution

There are many theories as to why lobe-finned fish adapted to amphibious lifestyles. Early hypotheses given in 1958 by A. S. Romer proposed that tetrapod evolution was driven by natural selection occurring when pools evaporated in arid conditions and left fish stranded (Romer, 1958). Some hypotheses propose that the evolution of limbs resulted from species migration due either to overcrowded niche space (Inger, 1957) or as a mechanism for avoiding predation by the large carnivorous fish of the Devonian (McNamara and Selden, 1993). Clack (2002) suggests that because of the high diversity of fish, the radiation of plants onto land, and the subsequent infestation by land arthropods, the terrestrial realm was a wide-open niche space waiting to be filled.

The evolution of terrestriality in tetrapods is not well resolved but is likely driven by the environmental changes in global and local climates brought on by plants, which impacted the animal's morphology, behavior, and respective niche space. Many theories have evolved around the dramatic impact on global climate and terrestrial environments caused by the colonization and radiation of land by plants. Early plants accelerated the weathering of the substrate in which they were rooted, transforming rock into nutrient-rich soils. Fluvial processes interacting with regolith created more freshwater habitats for emergent species (Algo and Scheckler 1998; Berner, 2009). George and Blieck (2011) suggested that the environmental conditions created by land plants played a major role in the emergence of tetrapods, due to increased atmospheric oxygen.

Devonian to Carboniferous climate

As tetrapods diverged from lobe-finned fish in Frasnian, the earth was in a hothouse climate with an average global temperature around 20˚C that rose to 24˚C at the

time of the Kellwasser thermal maximum (373 Ma) (Scotese, 2021). For comparison, modern globally averaged temperatures are 14.8 ˚C, 1.1˚C warmer than estimated pre-industrial (1880) values (NOAA, 2022). Although the cause of the Kellwasser thermal maximum is not generally agreed upon (some studies suggest weathering and increased atmospheric oxygen released by expanding populations of land plants, volcanism, tectonic events, and even extraterrestrial body impacts (Le Hir et al., 2011; McGhee et al., 1986; Ricci et al. 2013)), the Kellwasser Event led to rapid warming and cooling over the next million years or so. Throughout the remainder of the Famennian, the interval when the early tetrapods became more adapted for amphibious lifestyles, temperatures stayed warm (~23˚C). Global average temperatures began to drop from 23˚C at the end of the Famennian, to 19˚C in the early Carboniferous leaving the world in an ice age (Scotese et al., 2021; Streel, 2002). At this time many tetrapodamorphs populated equatorial regions, thriving in warm environments (Clack, 2002).

The Serpukhovian (331 to 323 Ma) marks the beginning of a consistently cool global climate phase with temperatures below 18˚C. The climate remained cool (around 13˚C) for much of the Pennsylvanian with ice caps forming at the poles during the Bashkirian and ice volume and sea levels being controlled by Milkovich cycles in Moscovian (Scotese et al., 2021; Streel, 2002). Although the climate was cool, tetrapods maintained a foothold in the tropics, living among lycophyte dominated forests, deltas, and swampy lakes (Daeschler, 1995; Clack 2002; Falcon-Lang et al., 2010).

Study sites

One of the best paleontological windows on the evolution of tetrapodamorphs is preserved in the road-cut exposure of the Devonian red beds located in Red Hill,

Pennsylvania (Figure 2). Due to the abundance and variety of well-preserved, late Devonian tetrapodamorph fossils representing a wide range of the fish and amphibian found here, the site has been extensively studied. Previous work on the site includes stratigraphic analyses (Peterson, 2010; Woodrow et al., 1973), faunal descriptions, and environmental reconstructions (Cressler et al., 2010; Daeschler et al., 2000, 2009). These allied studies provide an excellent independent constraints on the paleoenvironmental inferences which are made for the site based on $\delta^{18}O$ measurements of different taxa.

The second study site, the Joggins Formation, outcrops in Joggins, Nova Scotia (Figure 2) which preserves the oldest reptile *Hylonomus lyelli* (Dawson and Lyell, 1859) . That is, the Joggins Formation contains the first specimen thought to have the ability to reproduce in fully terrestrial settings. Although less anatomically dramatic than the evolution of legs from fins, the evolution of amniotic eggs was an equally important trait to have for tetrapods to colonize terrestrial inland environments. Because of the exceptional preservation of *in situ* flora and fauna, the site has been named a UNESCO World Heritage Site. Previous work on the sites includes stratigraphic analyses (Davies et al., 2005), geochemical analyses (Brand, 1994), faunal descriptions, and environmental reconstructions (Carpenter et al., 2015; Dawson, 1882; Grey 2011; Stimpson et al., 2012).

Both the Red Hill outcrop and Joggins Formation have been interpreted as lowland fluvial and adjacent floodplain, lacustrine, and/or swampy environments. Especially for the Joggins Formation, the degree of marine influence and the source region of surface waters to the site have been considered (Falcon-Lang, 2010; Grey et al. 2011; Tibert and Dewey, 2006), but for this site isotopic data that might test and refine

interpretations are limited (Brand, 1994), and similar data for the Red Hill roadcut are absent. In this study, we use $\delta^{18}O$ values of phosphatic fossils specifically to estimate the extent of marine influence through the Joggins section and examine alternative hypotheses for the moisture balance and possible habitat segregation at the Red Hill roadcut.

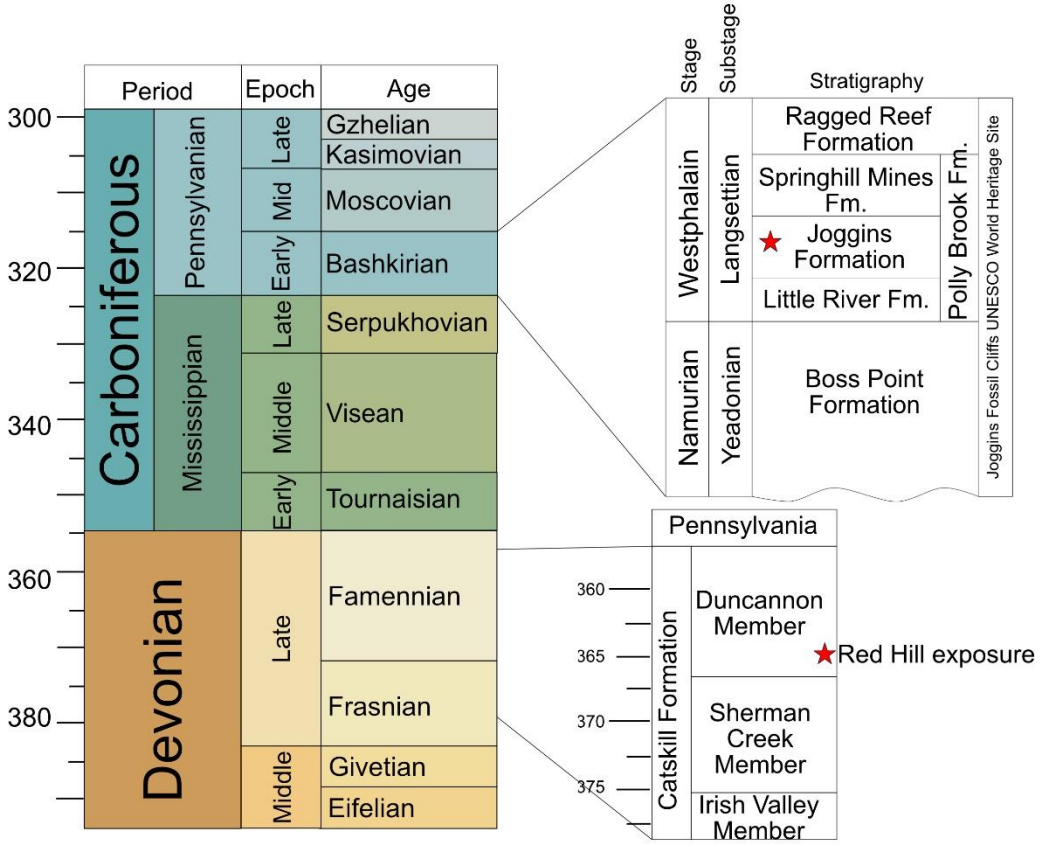

Figure 1: Devonian and Carboniferous geological and stratigraphic time scale modified from Harland et al., 1990; Daeschler and Cressler,2011; and Rygel et al., 2014.

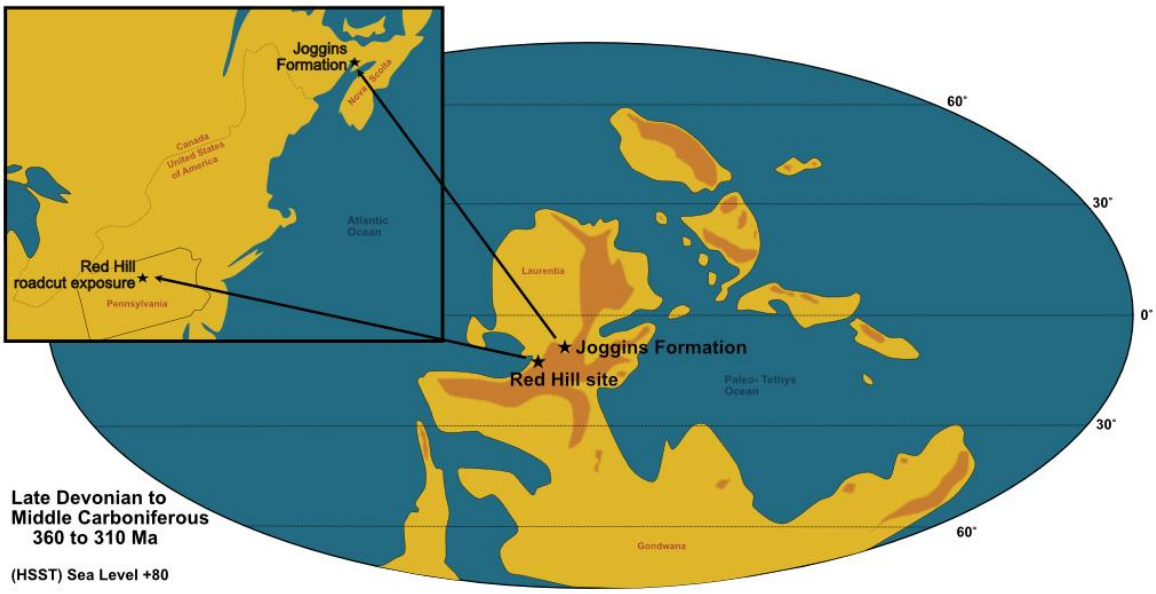

Figure 2: Map of the modern and ancient location of the Joggins Formation and Red Hill site. The Red Hill site and Joggins Formation are marked with black stars on the paleo map. The locations are marked on the paleo map modified from Scotese (2014) for the Visean (332.5) time which marks the midpoint between the formation of both outcrops. The modern location of the Joggins Formation and Red Hill site are marked with stars in the black rectangle inset.

Background: Red Hill, Pennsylvania

The Red Hill outcrop is a ~1 km long road cut the exposure of the Duncannon Member of the Catskill Formation located in Clinton County, Pennsylvania. The outcrop is exposed on PA route 120, 1.5 km west of Hyner, Pennsylvania, and represents a terrestrial floodplain ecosystem (Cressler et al., 2010; Peterson, 2010). Palynological results date the outcrop to the Upper Famennian substage with an estimated age of 361 Ma (Traverse, 2003) (Figure 1). At the time of deposition, Red Hill was located 20° south of the equator in the subtropical zone (Cressler, 2006).

Temperature variability

The expected temperatures for a subtropical lowland setting in the Famennian at a site like Red Hill range from 32- 38°C (Brand, 1993; Grossman, 2022; Scotese, 2021). Brand (1993) calculated Famennian subtropical shallow sea temperatures ranging from 32 to 38˚ C. Grossman et. al (2022) suggest an average temperature for latitudes between 30° S and 30° N to be 36.5°C. Scotese (2021) reported an average global temperature of 35°C for the time interval (361 Ma) consistent with palynological dates provided in Traverse (2003). Temperatures across the Red Hill floodplain were likely more variable than the proposed 32 to 38˚C due to seasonality and locally variable floodplain conditions (Amoros and Bornette, 2002; Trego, 2014).

Paleoclimate

Paleoclimate reconstructions based on sedimentological and paleontological evidence suggest seasonal changes in water levels strongly affected the flora and fauna at Red Hill. Seasonality is suggested by the presence of evaporates preserved within paleosols, charcoal layers associated with forest fires, and plant adaptations consistent

with deciduousness (Cressler, 2006; Cressler et al. 2010; Woodrow et al., 1973). Further, the presence of abundant shrink-and-swell clays in paleovertisols as well as silt deposits stacked above and below the plant layers at Red Hill are indicative of a seasonally wet and dry climate (Cressler, 2006). Cressler et al. (2010) suggest that the charcoal layers are indicative of frequent fires scorching the forests made vulnerable by dry conditions (Cressler, 2010). The presence of deciduousness in some trees, like the shedding of penultimate branches in *Archaeopteris,* may be an adaptation to extended dry periods (Scheckler, 1978).

Seasonal variation in the floodplain had a significant impact on (1) the availability of aquatic and terrestrial habitats, as well as the floral and faunal inhabitants, (2) the frequency of fires, and (3) the shape and flow of the channel (Cressler, 2006; Deschler et. al, 2011; Peterson, 2010; Trego, 2014). Due to the higher levels of precipitation in the wet season, the size of floodplain waterbodies increases, creating connections between the main channel and other floodplain waterbodies (Sullivan and Watzin, 2009; Trego, 2014). Similarly, due to reduced water levels in the dry season, ponds might have shallowed or dried out, reducing connectivity between the main channel and waters ponded on the floodplain (Cressler; 2006).

Species distribution

The seasonal wet and dry periods and resulting water levels controlled many aspects of life at Red Hill including the distribution of animal species (Cressler, 2006; Cressler, 2010). As such, some of the fish species found at Red Hill were restricted to certain areas of the floodplain based on the size and lifestyle of the animals (Trego, 2014) (Figure 3). *Hyneria lindae* (Thomson, 1968), the most common fish species found at Red

Hill, most likely lived in the main channel to accommodate for its size and carnivorous diet, (Cressler, 2010). Smaller species (between 30-100 cm) of fish like the megalichthyids and rhizodontids were suited to live in both the channel and in ponded water habitats (Cressler, 2010). Medium sized ray-finned fish such as *Gyracanthus* likely inhabited the shallow pond environments in the Red Hill floodplain (Cressler, 2010). Placoderms like *Turrisaspis elector* (Daeschler et al. 2003), were small (20 cm) and feasted mainly on detritus making them suited to a variety of environments. (Cressler, 2010; Trego, 2014).

As fish dominated the aquatic niche space at Red Hill, early tetrapods at the site were exploiting shallow water and semi-terrestrial habitats. The restricted shallow water habitats preserved at Red Hill likely provided a haven for early amphibians. Tetrapod fossil specimens found at Red Hill are very rare and are represented by isolated skeletal remains (Daeschler et al., 2009). Although fossil material is limited, the material shows a range of animal sizes, ornamentation, and morphology. Most of the specimens found at Red Hill are thought to have come from either of the two named species *Hynerpeton bassetti* and *Densignathis rowei (Daeschler et al., 1994)* or a still unnamed amphibian (sister taxa of icthostegalians) from the outcrop (Daeschler et al. 2009). Early amphibians like *H. bassetti* were well suited to life in the shallow fluctuating waterbodies on the floodplain (Cressler, 2010). However, while shallow water habitats disconnected from the main channel may have provided an effective escape for early amphibians from large and fast swimming predators like *Hyneria lindae,* it is likely the Red Hill amphibians were capable of moving among the different areas of the floodplain (Cressler, 2010).

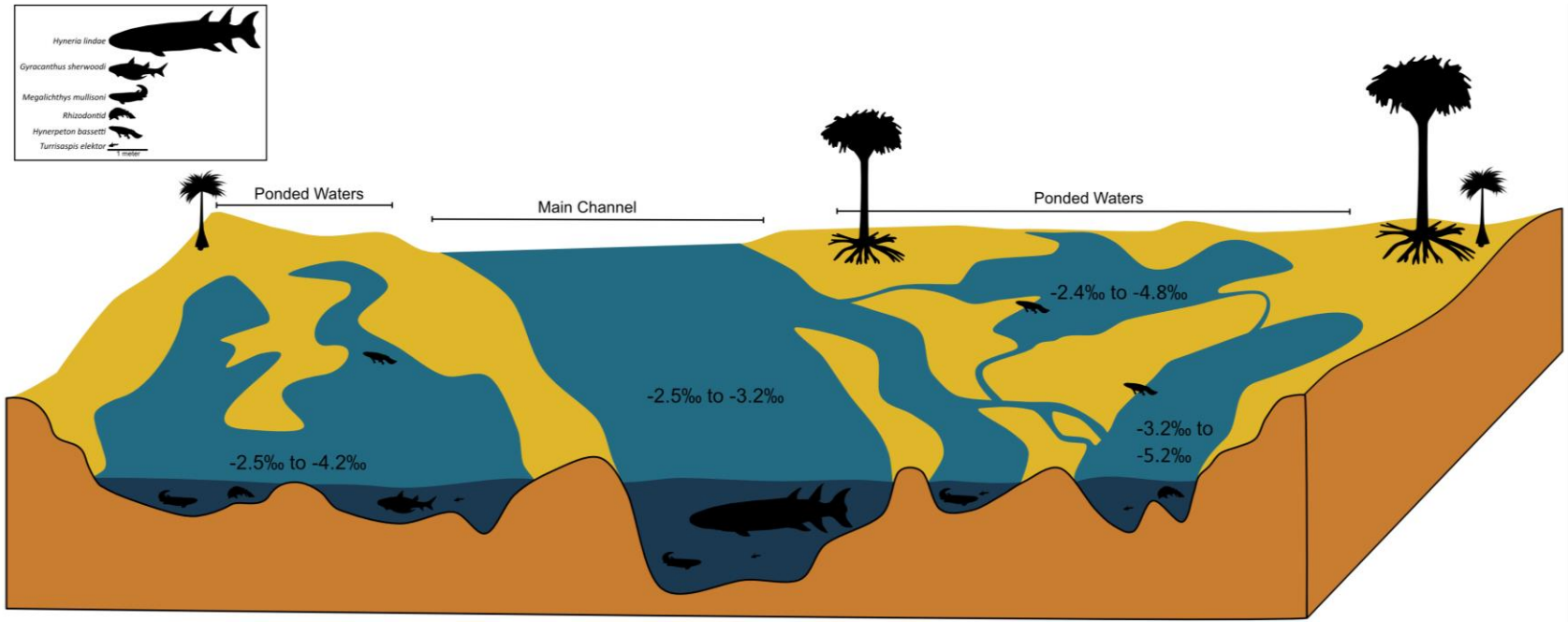

Figure 3: Floodplain habitat reconstruction with associated average $\delta^{18}O_{water}$ values. Organisms, marked with an associated icon which can be found in the key, are located in the part of the channel in which they lived (as specified by Cressler et al., 2010). The $\delta^{18}O_{water}$ value overlaying the water bodies is calculated from the average $\delta^{18}O$ of only the organisms found to have lived in the specific location. For example, the main channel $\delta^{18}O$ range is calculated only from the main channel taxon $\delta^{18}O_{phosphate}$ from Hyneria lindae*, and not from organisms suited to both the main channel and the ponded waters. Ponded water $\delta^{18}O$ is indicated within the ponded water section on the bottom far left (-3.7 to -4.8‰), main channel $\delta^{18}O$ (-3.0 to -4.3‰) is within the main channel section in the lower center, $\delta^{18}O_{water}$ from taxa suited to both the main channel and the ponded waters is indicated within the partially connected/ crevasse splay section on the bottom right (-4.2 to -5.6‰), and the $\delta^{18}O_{water}$ calculated from amphibian $\delta^{18}O$ is indicated within the crevasse splay section on the upper right (-3.7 to -5.0‰). Note: organisms in the floodplain diagram are not to scale, but organism markers in the key are.*

Background: Joggins Fossil Cliffs, Nova Scotia

The Joggins Fossil Cliffs are located in Nova Scotia, Canada along the Bay of Fundy. The Joggins Fossil Cliffs is a UNSECO World Heritage Site recording 15 million years of deposition (341 to 289 million years ago). The Joggins Fossil cliffs expose (from youngest to oldest) the Ragged Reef Formation, the Springhill Mines, the Joggins Formation, the Little River Formation, and the Boss Point Formation (Davies et al., 2005). These Formations are all within the larger Cumberland Group and were deposited in the Cumberland Basin. Palynological analyses conducted by Dolby (1991) date the 915.5-meter-long coastal exposure of the Joggins Formation to around 310 million years old (Davies et al., 2005).

Paleoclimate

Paleoclimatic interpretations for Joggins Formation indicate that sediments of the Joggins Formation were deposited in tropical conditions (within 5˚ of the equator) (Scotese Paleomap project). The expected temperatures for an equatorial lowland setting in the Mid. Carboniferous, like that preserved within the Joggins Formation, range from 20- 30˚ C (Brand, 1994; Grossman, 2022; Roseneau and Tabor 2013; Scotese, 2021). Based on oxygen isotopic analysis of 6 bivalves from the uppermost calcareous shale of the Joggins Formation, Brand (1994) estimated the paleotemperature of water ranged from 20-30˚ C . Similarly, Roseneau and Tabor (2013) indicate that equatorial sites from the Lower to Middle Pennsylvanian likely had temperatures ranging from 20 – 26˚ C, and Grossman (2022) proposed an average temperature of around 28˚ C for sites within 30˚ of the equators.

Overall, the Joggins Formation preserves three different types of floodplain conditions. Through sedimentological analysis, Davies et al. (2006) determined that the water level in the basin and resulting environmental conditions cycled as a function of glacio-eustatic sea level changes as well as local tectonism. The Joggins Formation is divided into 14 cycles of sea level rise and fall recorded in stratigraphic intervals which transition from open-water (ranging up to a few tens of meters deep), poorly drained coastal floodplains, and well-drained alluvial floodplains (Davies et al. 2006; Davies et al., 2005; Falcon-Lang et al., 2006; Falcon-Lang et al., 2004).

Units representing the poorly drained floodplain facies reflect a swampy environment supporting a wide variety of terrestrial and aquatic organisms including trees, insects, terrestrial gastropods, tetrapods, the earliest known reptiles, as well as aquatic and or marine bivalves and eurypterids (Falcon-lang et al., 2006). The poorly drained floodplain facies reflect a dryland terrestrial ecosystem which supported a variety of trees, ferns, tetrapods, gastropods, and arthropods (Falcon-Lang, 2003). *In situ* cordaitalean and lycopsid trees are the most abundant plants in the terrestrial settings and many occurrences of well-articulated tetrapod remains are preserved within the trees, giving the name “Hollow Tree Taxa” (Dawson, 1882; Falcon-Lang et al., 2006). The abundance of charcoal in the terrestrial facies suggests that fires frequently scorched forests perhaps diving amphibious tetrapods and early reptiles to take shelter in hollow trees (Falcon-Lang et al., 2006).

The open water facies association (OWFA) represents brackish to fresh low energy lacustrine habitats (Davies et al., 2004). Fossilized taxa present in the OWFA facies include bivalves, ostracods, foraminifera, echinoids, and a few species of

encrusting tube worms (Falcon-Lang et al., 2006; Grey, 2011). Vertebrate fossils in this facies include several species of fish and icthostegalian tetrapods. While lobe-finned fish and tetrapods were suited to both freshwater and marine habitats, the presence of some marine to estuarine taxa within the Joggins Formation suggest the waters were brackish.

Marine contribution

The marine influence on the Joggins Formation has long been a topic of study. Calder (1998) and Tibert and Dewey (2006) suggest that during periods of high sea level the Tethys Ocean occasionally reached the Cumberland Basin waters (through a hypothetical seaway). Due to the mid-continental palaeogeographical location of the basin in which the Joggins Formation was deposited with a large distance to the Tethys Ocean (Figure 2), marine waters likely mixed with the freshwater runoff in the Cumberland Basin, but retained sufficient salinities likely to support brackish taxa (Calder, 1998; Tibert and Dewey, 2006). Brackish and or marginal marine taxa such as ostracods, eurypterids, horseshoe crabs, shrimps, horseshoe crab tracks, foraminifera, rays, and sharks appear in bituminous shell beds located around ~550 and ~570m above the base of the Joggins Formation (Falcon-Lang, 2010). Echinoid fragments are preserved in the Formation (0 to 550 meters from the base) and appear to decrease in abundance up section (Grey et al., 2011). This observation suggests that marine influence was prominent in the first half (around 500 m) of deposition of the Joggins Formation, but that the influence of marine water decreased over time (Grey et al., 2011).

The degree of marine influence can be constrained by coupling the presence of marine and or brackish and freshwater taxa with other environmental proxies. However, geochemical analyses on bivalves from the uppermost calcareous shale horizon at the

Joggins Formation don't suggest marine conditions (Brand, 1994). Using strontium isotopes Brand (1994) indicates the geochemistry of the bivalves reflects aquatic/nonmarine conditions consistent with a continental setting. Similarly, oxygen isotopic measurements indicate that the waters of the Cumberland Bain during the deposition of the Joggins Formation had an $\delta^{18}O$ value of -5.5 to -2.3 ‰ $_{VSMOW}$ which is much lower than the expected value of seawater (~1‰ during glacial times) suggesting the clams lived in freshwater (Brand, 1994). The analysis done in Brand (1994) aligns with the conclusions drawn by Grey et al. (2011), supporting the model for decreasing marine influence up-section.

Technical History

Palaeothermometry

Oxygen isotope palaeothermometry is based on the temperature dependent fractionation of ^{18}O and ^{16}O between a mineral and the solution from which it formed. The oxygen isotopic composition of water preserved in phosphate minerals is reported in parts per thousand (‰) relative to the oxygen isotopic composition of modern mean seawater values, specifically relative to Vienna Standard Mean Ocean Water (VSMOW) (Sharp, 2017). The magnitude of the fractionation is temperature dependent; as temperature increases, the degree to which the isotopes fractionate decreases (Sharp, 2017). In general, an increase in temperature by 1 °C corresponds to a decrease in $\delta^{18}O$ by 0.22‰ (Streel, 2000). Because the relationship between temperature and isotopic ratios is well constrained, assuming formation of mineralized sample in equilibrium with local waters, the isotopic ratio of a mineral, or of mineralized tissue can be used as a proxy for temperature.

Carbonate and phosphate bioapatite have both been used in paleotemperature studies. Diagenesis, postmortem alteration of remains resulting in shifts from the initial isotopic ratio, has been shown to affect carbonate more than phosphate (Schoeninger and DeNiro, 1982; Wenzel et al., 2000). Carbonates are generally preferred for isotopic analysis, but due to their resilience to diagenetic overprinting, phosphate oxygen is often used for paleotemperature studies.

The phosphate paleothermometer is based on the relationship between the oxygen isotopic composition of phosphate ($\delta^{18}O\ PO_4^{3-}$) in biogenic apatite ($Ca_5(PO_4, CO_3, F)_3(OH, F, CL, CO_3)$) and water temperature (Kolodny et al., 1993; Lécuyer et al., 2013;

Longinelli and Nuti, 1973; Pucéat et al., 2010). The following equation is used to calculate the paleotemperatures based on two unknowns, (1) the temperature at which the mineralized tissue formed and (2) the isotopic composition of water at the time of formation.

$$T^{\circ} C = 117.4 - 4.50 * (\delta^{18}O_{\text{Phosphate}} - \delta^{18}O_{\text{Water}})$$

(Lécuyer et al., 2013)

Fractionation Processes

It is well known that there are several fractionation processes that can affect the second unknown, $\delta^{18}O_{water}$. The $\delta^{18}O$water of a waterbody is determined by the isotopic composition of the source water. For example, marine water has a $\delta^{18}O$ of around 0 per mil, while freshwater has generally lower $\delta^{18}O$ values. The $\delta^{18}O$ of water vapor is lower than the $\delta^{18}O$ of the marine water it came from due to fractionation occurring during evaporation and precipitation. When water evaporates, lighter isotope ^{16}O is concentrated in the vapor phase. Conversely water with the heavier isotope ^{18}O is preferentially partitioned into liquid that condenses from the vapor (Gat, 1996; Sharp, 2017). Because of this, when water vapor condenses and falls as precipitation, the $\delta^{18}O$ of the precipitation is higher than that of vapor. As more water is removed as precipitation, the $\delta^{18}O$ of the remaining vapor decreases as does subsequent precipitation. Similarly, the water remaining in a waterbody after evaporation is left enriched in the heavier isotope (oxygen 18). In this way, progressive evaporation can increase the $\delta^{18}O$ of the remaining water.

Marine water generally has a higher $\delta^{18}O$ than freshwater, ranging from 1 to -1 ‰. Evaporation, precipitation, freshwater contribution, and freezing can affect the $\delta^{18}O_{seawater.}$ Generally evaporation, precipitation, and the input of freshwater are buffered by the large volume of water retained in the ocean, with the oceans maintaining a $\delta^{18}O$ value around 0‰ (Sharp, 2017). Freezing, present as glacial ice at the poles, is different from the other processes. The removal of water vapor to continental ice sheets results in a 1‰ increase in the δ18O seawater over a few thousands of years (Sharp, 2017). The same is true for melting, whereas continental ice decreases, the $\delta^{18}O_{seawater}$ decreases by 1‰.

Diagenetic alteration can also alter the $\delta^{18}O$ value, resulting in generally lower $\delta^{18}O$ values of biogenic apatite in marine fossils (Wenzel, 2000). Diagenesis refers to the physical and chemical changes that occur in sedimentary rocks and fossils after they are buried. Chemical exchanges between the minerals and fluids in the rock lead to changes in the oxygen isotopic composition which reflect the temperature during the alteration of the minerals, but not at the time of original deposition (Lécuyer et al., 2013).

History of techniques used for isotopic analysis.

The technique for oxygen isotope analysis of phosphate was initially developed by Tudge (1960), who isolated PO_4 as $BiPO_4$, from which oxygen could be extracted by reaction with BrF_5 and converted to CO_2 for isotopic analysis. Longinelli et al. (1973) and Kolodny et al. (1983) refined this method and demonstrated its utility in the analysis of oxygen isotopes. However, the Tudge (1960) method has some limitations: the chemical procedures used to extract and purify the phosphate precipitate are complex and

time-consuming, and $BiPO_4$ is hygroscopic, so adsorbed water must be removed before fluorination, which can alter the isotopic composition of the phosphate if not done well.

Firsching (1961) developed a simpler and cleaner method for analyzing oxygen isotopes by isolating the PO_4^{3-} anion by precipitating Ag_3PO_4 to determine $\delta^{18}O_{phosphate}$. Wright and Hoering (1989) combined Firsching's technique with HF dissolution and the standard BrF_5 extraction procedure to improve the extraction of phosphatic oxygen for isotopic analysis. This method was further refined by Crowson et al. (1991) and Lécuyer et al. (1993), who found that fluorinating Ag_3PO_4 at a higher temperature and for shorter times improved the precision of the isotopic analyses. O'Neil et al. (1994) generally followed the same procedure proposed in Firsching (1961), but O'Neil et al. (1994) was the first to thermally decompose Ag_3PO_4 in the presence of graphite to produce CO for isotopic analysis. Modern studies often employ a modified version of the protocol proposed in O'Neil et al. (1994) and subsequent refinements, to isolate the PO_4 anion as Ag_3PO_4 and measure the $\delta^{18}O$ of biogenic phosphate using a high-temperature conversion in an elemental analyzer coupled to a continuous flow isotope ratio mass spectrometer (Joachimski et al. 2009; Lécuyer et al., 2013; Wang et al., 2008).

Materials and Methods

Red Hill Samples Preparation

Fossil samples from 5 species of fish and 1 species of amphibious tetrapodamorphs from the Red Hill Pennsylvania samples were provided by Dr. Ted Daeschler from the collections of The Academy of Natural Sciences of Drexel University. The specimens are the lower jawbone and coronoid tooth of *Hyneria lindae*, 2 partial fin spines from *Gyracanthus sherwoodi*, 2 scales from *Megalichthys mullisoni*, 3 dermal plate fragments from *Turrisaspis elector*, and a partial cleithrum from an indeterminate sarcopterygian (possible rhizodontid) (Figure 4). The fossil material from amphibious tetrapods was 5 different teeth from *Hynerpeton bassetti* (Figure 4).

Powders of well-preserved tooth, scale, and/or bone material was milled from fossil samples with a Dremel tool at low speeds. For scale and bone, samples were drilled from different positions on the surface of the fossil (Figure 4). For tooth samples the different samples were generated by drilling progressively deeper into the tooth in the same location. Because tetrapod teeth mineralized from the middle outwards, this method of sampling can provide insight into local variation in $\delta^{18}O$ over the time the tooth grew. Another benefit of this sampling method is the ability to compare $\delta^{18}O$ values preserved in the dense cosmine (enamel) that coats the outer surface of the tooth and the less dense dentine which mineralized first.

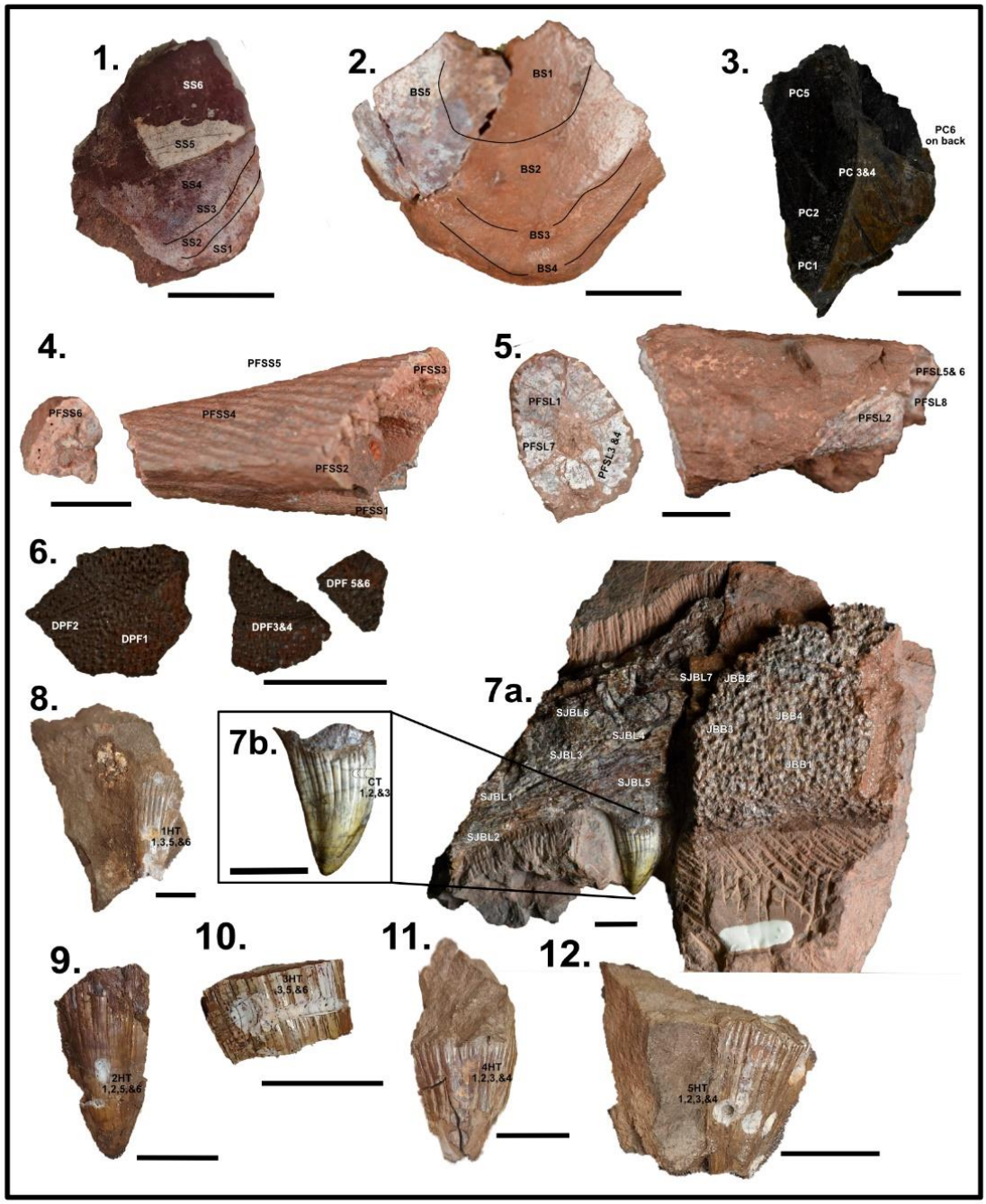

Figure 4: *Fossil material analyzed from Red Hill fauna. Drilling locations on each sample are marked in either black or white text. Scale bars for each image are 1 cm. Specimens are: 1. small scale from* Megalichthys mullisoni, *2. large scale from* Megalichthys mullisoni, *3. partial cleithrum from an indeterminate sarcopterygian (possibly a rhizodntid), 4. small partial fin spine from* Gyracanthus sherwoodi, *5. large partial fin spine from* Gyracanthus sherwoodi, *6. dermal plate fragments from* Turrisaspis elector, *7. Lower jaw and Coronoid tooth of* Hyneria lindae*; 7a. exposed section of jaw bone, 7b.. coronoid tooth, 8, 9, 10, 11, & 12. are isolated teeth from* Hynerpeton bassetti.

The Joggins Fomation samples preparation

The rock samples from the Joggins Formation were provided by Page Quinton, Michael Rygel, and Melissa Grey. Fifty-five samples from the Joggins Formation were used in this study. Of the 55 samples from Joggins, 21 were fossiliferous limestones, 31 were shales, and 2 were mudstones. The locations of collected samples is indicated on Figure 5.

Each bulk sample was first crushed to gravel size and then a portion was put in 1000 ml beakers. The sample weight was around 500g and ranged from 1000 and 100g. Selective dissolution or physical disaggregation was used to free the microfossils.

For the limestones, the material was soaked for 4 to 5 weeks (depending on dissolution progress) in a 10% glacial acetic acid (CH_3COOH) solution. Each week the samples were washed with tap water through a nest of sieves (1mm, 0.5 mm, and 0.15 mm). Insoluble material retained in the sieves was removed, saved in separate 500 mL beakers, and dried in an oven at 50˚C. Large pieces were returned to a refreshed 10% acid solution. Once dissolution was complete, all insoluble material saved throughout the dissolution was dried in an oven at 50˚C.

Shale samples were disaggregated using kerosene and “Sparkleen” manual washing soda (Sodium carbonate (Na_2CO_3), sodium dodecylbenzenesulfonate ($C_{18}H_{29}NaO_3S$), and non-ionic Detergent; (SPARKLEEN MSDS, 2013). Kerosene was added to the sample beakers containing 500 g of dried bulk material and left to soak for 24 hours. Excess kerosene was then poured off and a solution of 2 g of Sparkleen per liter water was added to disaggregate the samples. Shales disaggregated rapidly using this

procedure and the resulting sediment was washed in a three-tier sieve with tap water. The fossil-containing residues retained on the sieves were dried at 50°C in an oven.

For residues from both the limestone samples and the shale samples, vertebrate fossil material (bioapatite) was concentrated using a bromoform heavy liquid to separate the denser fraction of the material that should contain the bioapatite from less dense silicates and carbonates. The isolated dense fractions were again washed and dried at 50˚C. Microfossils were picked from the residues using a stereomicroscope.

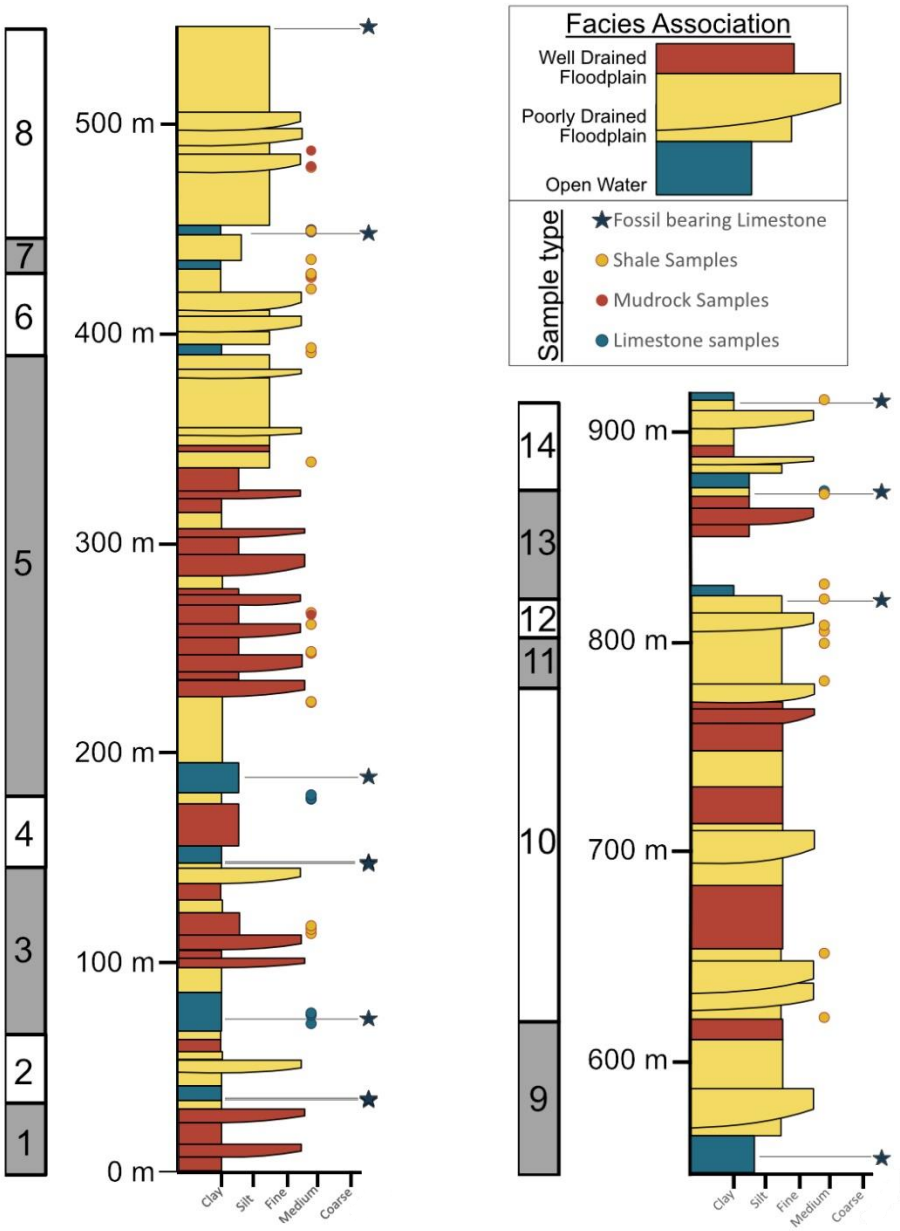

Figure 5: Stratigraphic column of the Joggins Formation modified from Grey et al. (2011). Following Grey et al.'s (2011) facies analysis, beds shaded in red represent well-drained floodplain environments, beds shaded yellow represent poorly-drained floodplain environments, and blue shaded beds represent open water environments. Glacio-eustatic facies cycles proposed by Davies et al. (2006) are marked from 1 to 14 in the lefthand column. Sample locations are marked with symbols (circles and stars) to the right of the stratigraphic column. Yellow symbols indicate samples from shale beds. Red symbols indicate samples from mud or siltstone beds. Blue symbols indicate samples from limestone beds. Circles indicate samples which did not yield enough fossil material for analysis. Stars indicate samples which yielded enough fossil material for analysis.

Analytical Procedure

Phosphatic microfossils from the Joggins locality and powdered tooth, bone, and scale samples from the Red Hill outcrop were prepared for isotopic analysis by isolating the PO_4^{-3} anion as Ag_3PO_4 using a technique modified from O'Neil et al (1994) and Lécuyer et al. (2004). Samples weighing around 1 milligram were loaded into 2 mL microcentrifuge vials and dissolved for 24 hours with 2M HNO_3 (0.087 ml per 1 mg sample). Subsequently, 2M KOH (0.030 ml per 1 mg sample) and 2M KF (0.048 ml per 1 mg sample) were added to the solution to increase pH and strip the Ca^{2+} cation from the solution by precipitating CaF_2. After 24 hours, these samples were centrifuged for 2 minutes at 10,000 rpm to separate the CaF_2 precipitate and any material not dissolved by the HNO3 from the solution. The supernatant (containing the dissolved phosphate) was transferred to a new vial. The insoluble residues were rinsed 3x with 0.050 ml of DD H_2O, centrifuged, and the rinse was added to the supernatant. A silver amine solution (2M NH_4OH (0.217 ml per 1 mg sample), 1M NH_4NO_3 (0.304 ml per 1 mg sample), and 1M $AgNO_3$ (0.174 ml per 1 mg sample)) was added to the supernatant. Samples were placed in an oven at 50˚C and as NH_3 slowly evaporated, the pH of the solution dropped, and Ag_3PO_4 crystals formed. The samples were removed from the oven after 24 hours, and the pH of the solution was tested to assure that the solution had reached a pH between 6.5 and 7.5 (indicating precipitation was complete). Samples were centrifuged for 2 minutes at 10,000 rpm. The supernatant was removed and discarded. Ag_3PO_4 crystals were washed with deionized H_2O 3 times and dried at 50°C and saved to await isotopic analysis.

Samples were analyzed at The Center for Stable Isotopes at the University of New Mexico in Albuquerque. Between 0.250 and 0.300 micrograms of dried Ag_3PO_4 crystals were weighed out on a Sartorius balance and transferred to silver capsules. Silver capsules containing the samples were crushed into small cubes and loaded into trays to await isotopic analysis. In addition to samples, weighed separates of international and internal standards (NBS 120c, IAEA Benzoic, USGS 80, USGS 81, and ARCOS) were also packed into silver capsules.

For analysis, samples were placed into the wells of a two-column automated carousel and dropped into the TC/EA reactor and decomposed. Standards NBS 120c, IAEA Benzoic, USGS 80, USGS 81, and ARCOS were analyzed concurrently to account for machine drift and to monitor for analytical precision. Evolved CO from all samples and standards was measured on a continuous flow Thermo Scientific Delta V Plus Isotope Ratio Mass Spectrometer over a three-day period. The isotopic composition was measured relative to a reference gas of known isotopic composition. Results are reported in delta notation relative to Vienna Standard Mean Ocean Water (SMOW). Because all samples were run within a three-day period, and measured values for international standards (USGS80, USGS 81, and IAEA Benzoic acid) were consistent over this interval (variation is ± 0.2‰), all samples were corrected with the same 3-point normalization using measurements of IAEA Benzoic acid, USGS 80, and USGS 81.

Data Correction

Raw data were corrected using a 3-point normalization based on regression of the average value of 7 to 8 replicates measured for three internal standards (IAEA 601 Benzoic Acid and apatite standards USGS 80 and USGS 81 analyzed at the start of the

runs). Nominal values for these standards are 13.1‰, 23.3‰, and 35.4‰, respectively. The equation used in the 3-point normalization was generated by plotting the accepted values of the standards against the values measured in this study. Corrected values for the average of multiple analyses of NBS 120c match the accepted value of 21.7 ‰, exactly confirming the accuracy of measurements. External precision is 0.4‰ (1 standard deviation) is reported based on replications of standards.

$\delta^{18}O_{water}$ estimates

In many studies, $\delta^{18}O$ is used as a proxy for temperature, due to the relationship between temperature and $\delta^{18}O_{phosphate}$. Several studies have proposed temperature equations to quantify the relationship between temperature and $\delta^{18}O$ (Kolodny et al., 1993; Lécuyer et al., 2013; Longinelli and Nuti, 1973; Puce´at et al., 2010). This study utilizes the temperature equation presented by Lécuyer et al. (2013).

$$T^{\circ} C = 117.4 - 4.50 * (\delta^{18}O_{Phosphate} - \delta^{18}O_{Water})$$

(Lécuyer et al., 2013)

To assess variation in the isotopic composition of the waters present through the intervals and among environments studied from each locality, we solved the phosphate paleotemperature for $\delta^{18}O_{water}$ (below) and evaluated the result for each sample across a range of temperatures expected given the age and setting of each locality.

$$\delta^{18}O_{Water} = \delta^{18}O_{Phosphate} - ((T^{\circ} C - 117.4)/ -4.50)$$

Modified from Lécuyer et al. (2013)

Red Hill Floodplain Groups

Taxa from the Red Hill roadcut are separated into 4 groups representing different habitats and aquatic conditions on the floodplain; (1) ponded water taxa, (2) main channel taxa, (3) taxa suited to either ponded waters or the main channel, and (4) amphibious taxa, based on Cressler's (2010) account of the habitats of specific taxa from Red Hill (figure 3). In our samples ponded water samples include the ray-finned fish *Gyracanthus sherwoodi* and the rhizodontid sarcopterygian (figure 3). The main channel fauna is represented by *Hyneria lindae*. Two taxa make up the taxa represented in either the ponded waters or the main channel: *Turrisaspis elector* and *Megalichthys mullisoni*. The amphibious taxa are represented by isolated teeth from *Hynerpeton bassetti*.

Seawater mixing model

Salinity estimates for the Joggins Formation were calculated using a simple mixing model. Using an estimate for $\delta^{18}O$ freshwater of -8.0‰ and an estimated $\delta^{18}O$ seawater of 1.0‰, the extent of marine influence is estimated using the calculated $\delta^{18}O$ of water at given section of the Joggins Formation. Using -8.0‰ as the freshwater endmember and 1‰ as the seawater endmember, the following equation is used to estimate % seawater (where 50% seawater corresponds to the midrange $\delta^{18}O$ value of -3.5‰)

$$\delta^{18}O_{mixwater} = (\delta^{18}O_{seawater} \text{ x proportion seawater}) + (\delta^{18}O_{freshwater} \text{ x proportion freshwater})$$

Where proportion of seawater + proportion freshwater = 1

The expected salinities for fresh and marine water are defined by the USGS Constraints on salinity as 0.5 (ppt) for fresh water and 34 ppt for seawater (USGS, saline water and salinity). In this model the salinity used for freshwater is the midpoint for freshwater, 0 ppt. Using the equation

$$\text{Salinity (ppt)} = (\%\ \text{seawater} \times 34\ (\text{ppt})) + (\%\ \text{freshwater} \times 0.5\ (\text{ppt}))$$

the overall expected salinity for any estimated $\delta^{18}O_{water}$ can be calculated for any section.

Results:

Red Hill, Pennsylvania

Measured $\delta^{18}O_{phosphate}$ on Red Hill samples range from 16.1‰ to 11.3‰ $_{SMOW}$. The average estimated $\delta^{18}O$ of water ranges from -6.3 to -2.8‰ when calculated for 32° to 38°C. The $\delta^{18}O_{water}$ values of the phosphatic fossils of the 12 organisms analyzed suggest neither a systematic negative moisture balance (net evaporation) nor a high degree of variability in moisture balance and or water sources among or within the four recognized sub-environments across the Red Hill floodplain.

Variability in $\delta^{18}O_{water}$ across the floodplain

There are small differences among isotopic values for taxa separated into the 4 facies groups described previously (ponded water taxa, main channel taxa, taxa suited to either ponded waters or the main channel, and amphibious taxa (Cressler, 2010)). Ponded water taxa yielded $\delta^{18}O$ phosphate values of 13.3 to 15.5 ‰, 14.8 to 14.2‰ (gyracanthus), and 12.7 to 15.1 ‰ (rhizodnt) (figure 4 and Figure 6). Analysis of material from the main channel taxon *Hyneria* yielded $\delta^{18}O_{phosphate}$ of 14.7 (±0.6) ‰. Taxa commonly found in both main channel and ponded waters facies yielded $\delta^{18}O_{phosphate}$ of 11.6 to 15.1 ‰ (*Turrisaspis)* and of 13.0 to 14.0‰ and 12.9 to 15.1‰ (*Megalichthys).* The samples of amphibious taxa yielded $\delta^{18}O_{phosphate}$ of 11.3 to 14.8 ‰, 12.9 to 14.8‰, 13.2 to 15.6‰, 13.7 to 14.6‰, and 14.3 to 15.6‰. Based on the habitat groups and annual temperatures of 32˚ to 38˚C, the ponded waters have a $\delta^{18}O_{water}$ value of -3.1 to –4.4‰, and the main channel $\delta^{18}O_{water}$ value is -3.0 to -4.3‰, potentially ponded or the

main channel waters yielded $\delta^{18}O_{water}$ -4.2 to -5.5‰, and the aqueous habitat of the amphibious taxa had an average $\delta^{18}O_{water}$ value of -3.7 to -5.0‰ (Figure 6).

Variability within individuals and sample types

Four different sample types (enamel, dentine, bone, and scale material) were analyzed in this study. Sampled enamel had an average $\delta^{18}O$ of 14.6‰, sampled dentine had an average $\delta^{18}O$ of 13.8‰, sampled bone had average $\delta^{18}O$ of 14.3‰, and sampled scale material had average $\delta^{18}O$ of 13.4‰. The enamel layers sampled in this study, in both *Hyneria* and the 5 *Hynerpeton*, had generally higher $\delta^{18}O$ than the non-enamel, dentine layers from the same tooth and bone samples from the same organism (when present). The difference between the average enamel $\delta^{18}O$ values and average dentine $\delta^{18}O$ (from the same tooth) ranged from 0.3‰ to 2.0 ‰ (Figure 4). *Hyneria lindae* was the only individual from which three different sample types were sampled. The difference in average $\delta^{18}O$ bone (14.3) and dentine (15.0) was 0.6‰. The difference in average bone and enamel (15.3) from *Hyneria* was 0.9‰.

Although some specimens exhibited considerable variation in values among samples (max = 3.7‰ for *Turrisapis*), there is no consistent pattern to the variability that might suggest a strong seasonal signal or directional ontogenetic shifts (figure 7). Sampling density within specimens is low, though (figure 4). The tooth $\delta^{18}O_{phosphate}$ from *Hynerpeton* tooth 1 had the second most variable $\delta^{18}O$ values, with a 3.5‰ difference from the enamel layer (14.8‰) to the core of the tooth (11.3‰). *Hynerpeton* tooth 2 yielded lower variability in $\delta^{18}O$ overall, but the values within the tooth were within 0.1‰ of the $\delta^{18}O$ values from *Hynerpeton* tooth 1 over the enamel to sub enamel

locations of the tooth. Enamel and bone sample values from *Hynerpeton* 3 ranged from 13.2 to 15.1‰ and are as variable as the other *Hynerpeton* teeth. *Hynerpeton* tooth 4 varied from 13.7 to 14.6‰, and *Hynerpeton* tooth 5 varied from 14.3 to 15.6‰. Enamel layers are 14.2 - 14.3‰, at the sub-enamel layer $\delta^{18}O$ increases to 14.5‰ for both teeth, at the outer core of the tooth, $\delta^{18}O$ drops by 0.8‰ (*Hynerpeton* 4) to 0.2‰ (*Hynerpeton* 5) and then increases by 0.9‰ (*Hynerpeton* 4) to 0.8‰ (*Hynerpeton* 5).

The $\delta^{18}O$ values from two scales from megalichthys range from 12.9‰ to 15.1‰ and 13.0‰ to 14.0‰. The outermost (oldest) concentric growth ring yielded 13.1‰ (big scale) and 13.4‰ (small scale), at the boundary of the second concentric ring $\delta^{18}O$ increased marginally by 0.1 to 13.5‰, the $\delta^{18}O$ from the second youngest ring dropped by 0.5 (big scale) and 0.6‰ (small scale), and the innermost and youngest sampling location on the scales increased to 14‰ for the big scale and 15.1‰ for the small scale.

The $\delta^{18}O$ of both tooth and bone material from *Hyneria lindae* ranges from 13.7‰ to 16‰ (Figure 7). The bone material has overall low variability ranging from 14.0‰ to 15.0‰, while the tooth material was more variable with values from 13.7‰ to 16.0‰. The enamel layer had the highest $\delta^{18}O$ value (16.0‰), the sub-enamel layer was 2.3‰ lower than the enamel, and the inner two layers of the tooth were 15.0‰ and 14.9‰ respectively.

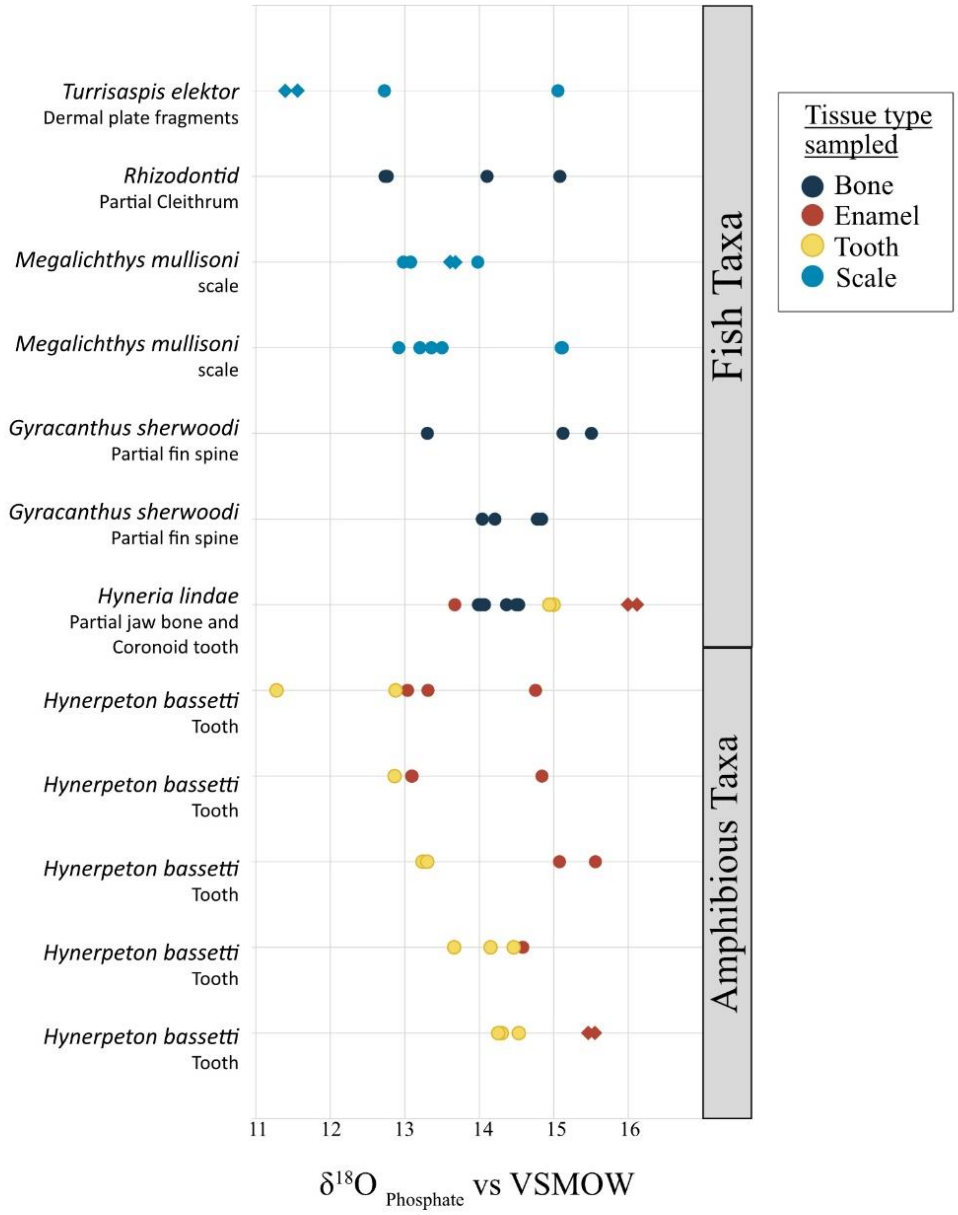

Figure 6: Plot of $\delta^{18}O_{phosphate}$ from organisms from the Red Hill floodplain. Animal species and type of fossil sampled is indicated on the left. The plot frames the $\delta^{18}O$ phosphate sampled from multiple locations on each fossil (sampling locations demonstrated in Figure 4). Sample types are indicated with different colored markers; dark blue for bone, red for enamel, yellow for non-enamel tooth material, and light blue for scales. Diamond markers are indicative of duplicates from the same location.

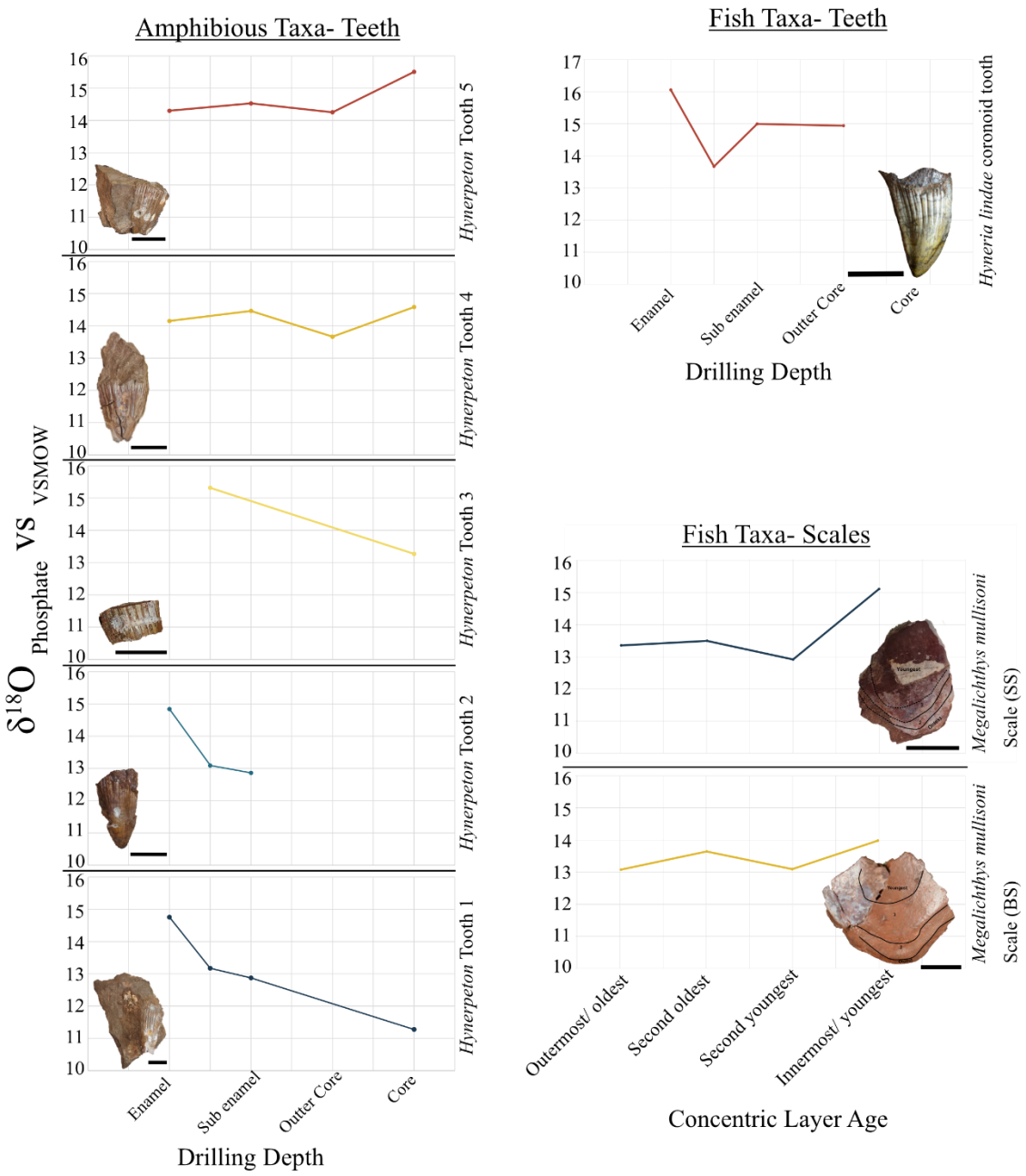

Figure 7: Left: Plot of $\delta^{18}O_{phosphate}$ values over the cross section of each Hynerpeton *tooth sampled. Duplicates from the same tooth depth have been averaged for this plot. Lower right: plot of $\delta^{18}O$ values over the cross section of both* Megalichthys mullisoni *scales sampled. Duplicates from the same scale layer have been averaged for this plot. Plot of $\delta^{18}O$ values over the cross section of Coronoid tooth from* Hyneria lindae. *Duplicates from the same tooth depth have been averaged for this plot. Scale bars are equal to 1 cm.*

The Joggins Formation, Nova Scotia

Sufficient abundances of phosphatic fossils for isotopic measurements were recovered in 12 of the 54 samples processed. The $\delta^{18}O_{phosphate}$ values of these samples range from 16.4‰ to 12.3‰ (Table 2, Figure 8). For the estimated temperature range of 20-30˚C proposed in Brand (1994), $\delta^{18}O_{water}$ values calculated using the temperature equation from Lécuyer et al. (2013) are -5.2 ‰ to -9.4‰ for temperatures of 20˚ C, and -3.0‰ to -7.1‰ for temperatures of 30˚C. These calculated values are much lower than the expected seawater values of ~1‰ expected for a time like the early Late Carboniferous when global ice volume was comparable to that of the Last Glacial Maximum (Scotese et al., 2021).

Calculated marine contribution

Using an assumed seawater value of $1‰_{SMOW,}$ and fresh water isotopic value of -8‰ estimated for a low latitude lake fed by precipitation and runoff from adjacent highlands, calculated $\delta^{18}O_{water}$ of -8.3 to -4.1‰ for local waters (at the temperature midrange 25˚C) during deposition of the Joggins Formation, suggests an average marine contribution of 20% and maximum marine contribution of 50% which reflects an average salinity of 7.2 ppt and a maximum salinity of 17 ppt (Figure 8). Further, for samples with the lowest estimated $\delta^{18}O_{water}$ for local waters (-9.4 ‰) would predict an average mixture of 0% marine waters and 100% fresh waters whereas the highest estimated $\delta^{18}O_{water}$ of for local waters (-3.0‰) would result from a mixture of 56% marine waters and 44% fresh water. Finally, assuming contemporary seawater had a salinity of 34 ppt and fresh water 0.5 ppt, the range of possible salinities for Joggins surface waters range from 0 to 17 ppt.

Variability between horizons is small, and consistent with the estimated temperature range. The following $\delta^{18}O$ values are calculated at 25°C the temperature range (20 to 30°C) midpoint of (Figure 8). Within the first 200 meters from the base, $\delta^{18}O_{water}$ ranges from -6.6‰ at 35.5 meters from the base to -7.8‰ at 189 meters from the base. None of the bulk rock units from 200 to 400 meters from the base yielded enough material for analysis. From 400 to 600 meters from the base $\delta^{18}O$ ranges from -7.9‰ at 448.4 meters to -6.5‰ at 547 meters, and -6.9‰ just 7 meters above at 554 meters from the base. Bulk rock units from 600 to 800 meters did not yield enough phosphatic material for analysis. From 800m to the top of the Joggins Formation, there was a moderate excursion where $\delta^{18}O$ increased from -7.3‰ at 820.3 m to -5.0‰ at 872 m and finally at 915.5 meters $\delta^{18}O$water is -6.8‰.

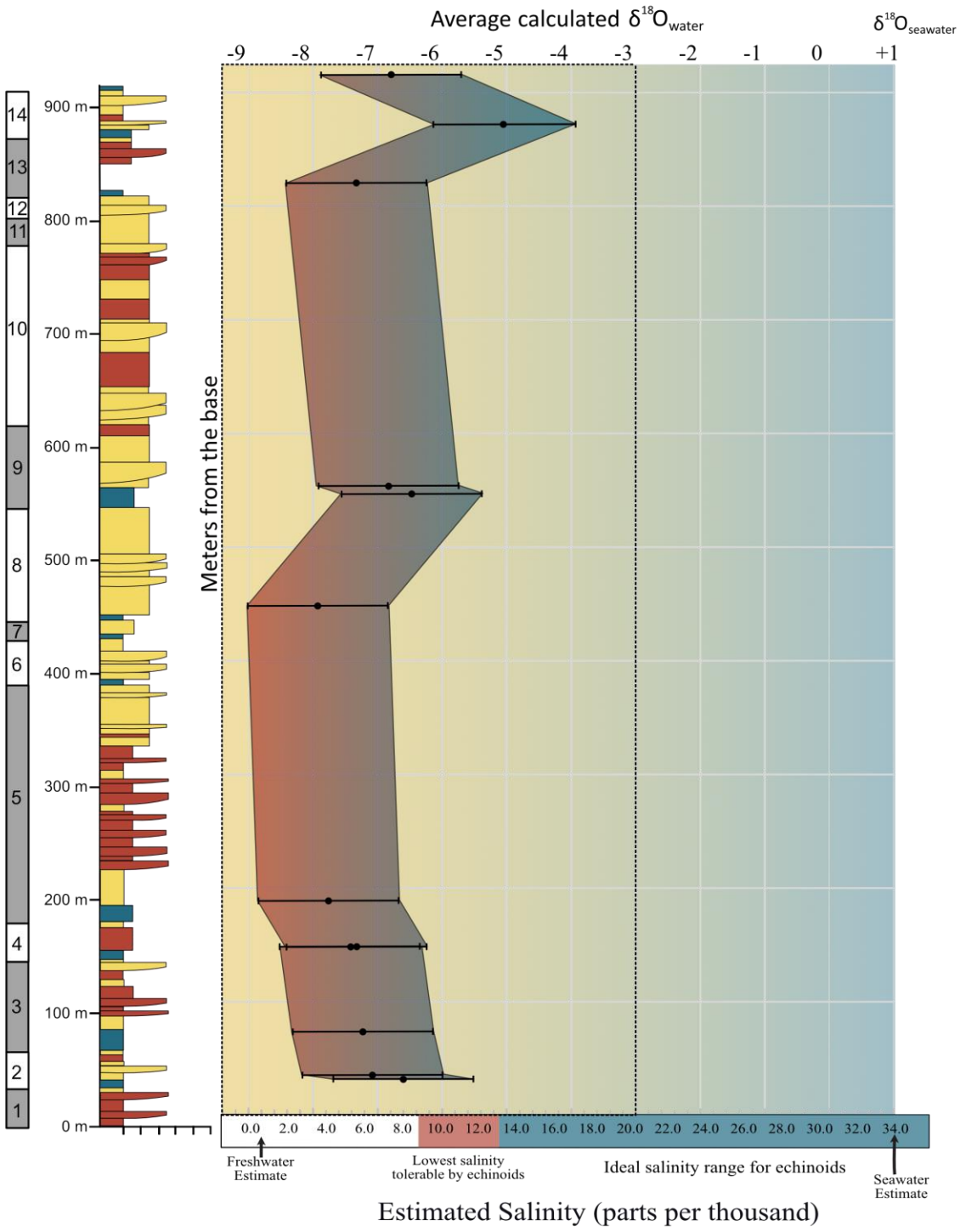

Figure 8: From left to right: (1) Glacio-eustatic facies cycles proposed by Davies et al. (2006). (2) Stratigraphic column of the Joggins Formation modified from Grey et al. (2011). (3) $\delta^{18}O_{water}$ of all duplicates over the measured section across the temperature range 20 to 30˚C. (4) The black box with dashed border indicates the maximum range of $\delta^{18}O_{water}$ values for temperatures of 20 to 30˚C at Joggins. (5) Bar on the bottom indicates the estimated salinity based on the marine mixing model (6) colored sections of the bar indicate the salinity tolerances of echinoids.

Discussion Red Hill, Pennsylvania

Possible explanations for the lack of evidence for evaporation:

The observed record of $\delta^{18}O_{water}$ suggests that the Red Hill floodplain was not strongly influenced by evaporation. That is, similarity in the calculated $\delta^{18}O_{water}$ values within and among the different general floodplain waterbodies (ponded water, main channel, and amphibian habitat waters) suggests all areas of the Red Hill environment were fed by the same source water and sub facies experienced similar environmental conditions.

Sedimentological evidence for wet and dry seasons at Red Hill such as the presence of evaporates (present as caliche nodules), abundant shrink-and-swell, and occasional evidence of deciduousness in trees reflect dry seasons or episodic droughts. Ponded water facies should be more prone to evaporative drying than the main channel. It follows that, evaporation which would drive $\delta^{18}O_{water}$ values higher should be evident in the taxa living in the ponded waters. However, the calculated $\delta^{18}O_{water}$ values for the ponded waters are as high as any other $\delta^{18}O_{water}$ value in the floodplain. If anything, the wider range of values among ponded water taxa has more low values relative to the relatively narrow range of values measured on the jaw and tooth from *Hyneria lindae*.

Several possibilities exist to reconcile sedimentological and paleontological observations with $\delta^{18}O$ estimates. Discharge from floodplain ponds back to the main channel either through surface channels or groundwater infiltration during dry times may have occurred relatively fast, compared to $\delta^{18}O$ increases in ponded waters due to net evaporation. Thus, taxa living in these ponds would not experience extended intervals living in high $\delta^{18}O_{waters}$.

The generally low and variable $\delta^{18}O$ present in the mineralized tissue of *Turrisapis* implies conditions at times when storms introduced precipitation with low $\delta^{18}O$ values shifting values in marginal ponds without greatly affecting the main channel whose $\delta^{18}O_{water}$ value depended more on upstream tributaries fed by ground water discharge. Modern observations suggest temperature variability over a floodplain can range up to 17˚C (Amoros and Bornette, 2002). Considering such fluctuations, high temperatures and stormwaters filling ponds could explain the low values in some taxa. Temperatures calculated using the average $\delta^{18}O_{water}$ value (-3.9‰), $\delta^{18}O_{phosphate}$ generated in this study could reflect a temperature range of 49 to 27°C preserved over all the taxa sampled. While multiple fractionation processes may have been acting on floodplain waters concurrently, because progressive evaporation can increase $\delta^{18}O_{water}$ up to 50‰ (99% water evaporated), it has the potential to cause greater shifts in $\delta^{18}O_{water}$ than the temperature changes which result in $\delta^{18}O_{water}$ changing by ~1‰ for every 4˚C.

Alternatively, because animals typically grow tissue fastest when conditions are favorable, if droughts are stressful (e.g. reduced availability of food and nutrients, water anoxia or hypoxia, and decreasing habitat size) the formation of mineralized tissue in aquatic organisms would stop, and the evaporative signature would be unlikely to be recorded (Breitburg, 2002; Huang, 2021). Finally, $\delta^{18}O$ values of skeletal material is lower when temperatures are higher. Higher temperatures expected during times of net evaporation could lower the $\delta^{18}O$ values of mineralized tissue during droughts, masking the increase in the $\delta^{18}O$ values of the waters due to evaporation. These two possibilities are also not mutually exclusive.

Variability within organisms and sample types

Variability within and among the individuals sampled from the Red Hill roadcut is as high as 3.7‰, but the variability cannot be attributed to differences in sample types sampled. Overall variability of averaged $\delta^{18}O_{phosphate}$ for different sample types was low, with the maximum difference between sample types being 1.2‰. Generally, $\delta^{18}O_{phosphate}$ from enamel was higher than $\delta^{18}O$ dentine (0.3‰ to 2.0 ‰) and bone (0.9‰) (when present) from the same organism. However, this variability within sample types is small when the range of $\delta^{18}O$ over a single organism (with only one sample type sampled) is as high as 3.7‰. This finding is consistent with previous studies on the oxygen isotope signatures of teeth by Horn et al. (2009) which demonstrate that there is no systematic difference in the $\delta^{18}O_{phosphate}$ of enamel versus that of dentine.

This finding suggests that the variability in the $\delta^{18}O_{phosphate}$ within a single organism reflects environmental variability over an individual's life. The resolution of the current study is low, but variability of up to 3.7‰ within an individual could result from changes in temperature and the input of meteoric water and reflect seasonality. Previous sclerochronological studies on fish tooth $\delta^{18}O$ (Guy et al. 2018) and fish otolith $\delta^{18}O$ (NOAA Fisheries, 2015) have sampled along growth rings to generate temporal data in order to constrain the age of modern (bronze age to recent) fish by determining the number of seasons in which the organisms mineralized new sample. Seasonal trends in $\delta^{18}O_{phospahte}$ are observed in both the otolith and tooth material with the difference in $\delta^{18}O$ between warm and cold periods of around 1-4‰ observed in otoliths, and 2 to 3.5‰ observed in the teeth (Guy et al., 2018; NOAA Fisheries, 2015). Guy et al. (2018) found

that the tooth phosphate $\delta^{18}O$ covered nearly the entire seasonal range for teeth formed in isotopic equilibrium with the expected temperature of lagoon water.

Future analyses of teeth and scales from the Red Hill taxa could provide better constraints on the timing, magnitude, and impact of fluxuating temperatures and water volume on the Red Hill flood plain as well as providing an age of the induvial sampled. Milling and analyzing tens of locations (oldest to youngest samples) from the teeth and scales of tens of animals living on the Red Hill floodplain, would provide a sufficient basis on which to suggest the presence of seasons.

Discussion: The Joggins Formation

Geochemical analysis of the Joggins Formation reflects a nonmarine setting. Calculated $\delta^{18}O_{water}$ over the Joggins Formation (-3.0 to -9.4‰) for temperatures ranging from 20 to 30°C reflects waters in the basin were sourced dominantly from precipitation through runoff and groundwater.

Compared to the $\delta^{18}O_{water}$ calculated from analyses of six bivalves in Brand (1994) (-5.5 to -2.3‰), the calculated $\delta^{18}O_{water}$ from this study is slightly low (-3.9 to -9.0‰) but consistent with the same temperature range (20˚ to 30˚C). Based on typical values for tropical regions, $\delta^{18}O$ generated in this study falls within a reasonable range for $\delta^{18}O_{water}$ and could be influenced by several factors, such as the amount and timing of precipitation, seasonal variability, and the degree of mixing with groundwater, which could affect the $\delta^{18}O_{water}$ (Gat, 1996; Sharp, 2017). The low $\delta^{18}O$ values calculated in this study support observations made by Ryan et al. (1991) and by geochemical analyses by Brand (1994) which suggest the Cumberland Basin was likely fed by waters originating in the adjacent highlands. Precipitation falling at higher altitudes and filling the basin as runoff and/ or groundwater may reflect the low $\delta^{18}O$ values present in the Cumberland Basin over the deposition of the Joggins Formation.

Freshwater dominance during the deposition of the Joggins Formation

Multiple studies have proposed the limestones in the Joggins Formation were formed in an inland lacustrine setting, where water mixed with marine water from the Paleo Tethys Ocean (Calder, 1998; Tibert and Dewey, 2006). The episodic presence of marine or brackish waters in the basin is supported by the presence of marine and/or

brackish taxa preserved within the Joggins Formation (ostracods, eurypterids, horseshoe crabs, shrimps, rays, sharks, horseshoe crab tracks, foraminifera tests, and echinoid fragments) present in the first 570 meters of the Joggins Formation (Falcon-Lang, 2010; Grey, 2011).

Because $\delta^{18}O_{seawater}$ in the Carboniferous was around +1‰ (Scotese et al., 2021), the input of marine waters would result in relatively higher expected $\delta^{18}O_{water}$ values due to the difference in the isotopic composition of the mixing waterbodies. Using a model for estimating salinity, where seawater has a $\delta^{18}O_{water}$ value of 1‰ $_{SMOW,}$ $\delta^{18}O$ fresh water is -9‰ (estimated for a low latitude lake fed by precipitation and runoff from adjacent highlands), and the percent marine water is estimated from the location of calculated $\delta^{18}O_{water}$ value relative to the two endmembers, the salinity at any given section measured in this study can be calculated based on an average ocean salinity of 34 and freshwater salinity of 0.5 ppt (Figure 8). Using this mixing model, $\delta^{18}O_{water}$ calculated at the temperature midpoint (25°C), has an average salinity of 7 ppt over the measured units and the upper salinity limit, 17 ppt, is reflected by $\delta^{18}O$ calculated at the highest temperature range.

The presence of unequivocal marine taxa (echinoids) in the first ~500 meters of the measured section (identified by Grey et al., 2011) is strictly representative of saline waters in the Cumberland Basin during the deposition of the Joggins Formation. Turner and Meyer (1980) reported that modern echinoids (brittle stars) can tolerate salinities no lower than 9-13 ppt without death or coma (defined as the cessation of burrowing and movement), while 17-38 ppt seemed to be an ideal salinity range. Assuming Carboniferous echinoderms had similar tolerances, the predicated salinity range for the

bottom half of the measured section (0.5 to 12 ppt) suggest local waters could have supported echinoderms. While the range of salinity for the first 500 meters of section where echinoids were found is on the low end of the livable range, this finding does not preclude acceptable conditions for echinoids, but rather suggests variable salinity in the Cumberland Basin during the deposition of the Joggins Formation, which is reasonable for a basin connected episodically with the ocean.

One interesting possibility is that the dissolution of evaporates in the subsurface elevated local salinity (Waldron and Rygel, 2005), without affecting the $\delta^{18}O_{water}$. Such a mechanism to increase salinity is not required as we calculate salinity ranges within the tolerances of reported taxa, but higher resolution sampling at the Joggins Formation with tighter correlation based on geochemical and paleontological data might reveal mismatches. In such a case, to discriminate among hypotheses, oxygen isotope analyses of rock units containing echinoderm fragments would provide $\delta^{18}O_{water}$ values consistent with the conditions in which the echinoids lived. If the resulting $\delta^{18}O_{water}$ is not consistent with partial marine mixing and a resulting brackish salinity within the livable range of echinoids when the echinoids are present, further examination into the plausibility of salinity brought on the by the dissolution of evaporites may be considered further.

The presence of (1) evaporite deposits which were withdrawn and resulted in subsidence of the basin over the deposition of the Joggins Formation, (2) fossilized saltwater/ brackish taxa, and (3) oxygen isotopic data from this study and Brand (1994) which reflect a non-marine lake mainly fed by low $\delta^{18}O_{water}$, suggests the influence of saline groundwater may have influenced overall salinity of the Cumberland Basin. Several meters of evaporites were present and being withdrawn during the deposition of

the Joggins Formation, according to sedimentological analyses by Waldron and Rygel (2005). Groundwater interactions with these evaporate deposits could have resulted in the dissolution of the deposits resulting in subsidence of the deposits and saturation of groundwater with salt. Groundwater containing dissolved evaporites would be saline but would not reflect the high $\delta^{18}O$ associated with seawater, rather the isotopic composition of the groundwater would reflect the $\delta^{18}O$ of local precipitation and runoff (Monjerezi et al., 2011). A similar scenario is demonstrated in modern day Tunisia, where saline groundwater, created by the dissolution of evaporite minerals, has a $\delta^{18}O$ groundwater value of -4.6 to -7.4‰ VSMOW, a precipitation $\delta^{18}O$ value of -4.5‰, and no indication of marine influence (Hamouda et al., 2013). Following the observations made in modern-day Tunisia, saline groundwaters, fed by precipitation and runoff, could have contributed to the salinity of the Cumberland Basin, without increasing the $\delta^{18}O_{water}$.

Oxygen isotope analyses which support a lacustrine environment and reflect basin waters fed mainly by meteoric water and runoff from the adjacent highlands coupled with strontium isotope values reflecting the continental affinity of source water found by Brand (1994), suggest that water in the Cumberland Basin may have been impacted by the addition of nonmarine saline water in the form of groundwater with low $\delta^{18}O_{water}$ values. While oxygen isotope data from this study reflect low $\delta^{18}O$, which is more consistent with meteoric water rather than seawater, the $\delta^{18}O$ values calculated are within a reasonable range for marine influence.

Independent constraints on the salinity the source of the waters mixing with the Cumberland Basin could be explored using strontium isotope analyses from across the stratigraphic section, especially at locations where brackish and/ or marine taxa are

found. Continental rocks typically have a higher proportion of radiogenic strontium-87, due to the weathering of older felsic rocks, while marine rocks have a higher proportion of non-radiogenic strontium-86, which results from the weathering of newer volcanic rocks and sea floor spreading. It follows that strontium isotope analysis may inform on the source of saline water within the basin, which could provide additional constraints on the contribution of marine water versus groundwater at locations with brackish taxa.

Future work

Because only 12 out of the 55 stratigraphic heights sampled yielded enough phosphatic material for analysis, further analyses of phosphatic fossils from the section could provide a higher sampling density across the formation and quantify marine influence. Further, oxygen isotope analyses on floodplain and terrestrial taxa (from the poorly- and well-drained floodplain associations) could provide constraints on environmental conditions present during the evolution of the first reptiles. Finally, the presence of echinoids is an absolute paleontological observation which suggests the brackish waters were present in the Cumberland Basin (range 9 to 38 ppt). The source of saline water can be attributed to the influence of marine water with an average salinity range of between 0 and 15 ppt in the basin, or potentially, the influence of groundwater made saline by the dissolution of subterranean evaporite deposits.

Conclusions

The variability in floodplain $\delta^{18}O_{water}$ calculated from taxa from Red Hill, Pennsylvania, ranges 1‰ (-4.2 to -3.8‰) and does show a signal expected for net evaporation over the floodplain waterbodies. Evaporative conditions may not be reflected in the mineralized sample of organisms at the times of the highest evaporation due to (1) environmental stress which can cause organisms to grow more slowly or not at all, (2) isotopic fractionation resulting from the higher temperatures ($\delta^{18}O$ generally decreases) which are expected during times of net evaporation ($\delta^{18}O$ increases) could mask the signature of both, and (3) regional decreases in water table height resulting in variable local water levels, but consistent $\delta^{18}O_{water}$ values.

Overall, the variability within and among the organisms in the Red Hill fauna seems more reflective of aquatic conditions over the organisms' lifetimes rather than artifacts related to sample types. The analyzed variability within and among sample types was low (1.2‰), especially compared to the greater variability present over a single sample type in a single organism (3.7‰). The Red Hill floodplain taxa may have been influenced by seasonal variability in temperature and precipitation like that proposed in Cressler (2006, 2010), but the variability within taxa could also be attributed to the local temperatures of the waterbodies and the amount of precipitation entering the waterbody. Future studies focused on high resolution sclerochronology of Red Hill taxa could provide constraints on the presence and degree of seasonal changes in environmental conditions affecting the floodplain.

At the time of deposition, the Joggins Formation, Nova Scotia, Canada, this study finds no evidence for fully marine conditions. Although the $\delta^{18}O_{water}$ values calculated in this study are consistent with an equatorial lacustrine setting fed mainly by precipitation and runoff, two scenarios are considered for the presence of unequivocal saltwater taxa. First, salinity models based on expected $\delta^{18}O_{water}$ values and salinity content for seawater (1‰ and 34 ppt) and freshwater (-9‰ and 0.5 ppt) suggest that marine influence over the deposition of the Formation could have resulted in a salinity as high as 17 ppt. Second, the presence of evaporites underlying the Joggins Formation at the time of deposition suggest if dissolved by groundwater (which would have a $\delta^{18}O_{water}$ value consistent with precipitation) and discharged into the local environment could have increased the salinity of the Cumberland Basin without increasing the $\delta^{18}O_{water}$ value of the water. Both scenarios could provide conditions in which echinoids could survive (9 to 38 ppt tolerance), but further analyses of isotopic data reflecting the degree of marine influence are needed to constrain the salinity and exact source of saline water mixing with the Cumberland Basin during the deposition of the Joggins Formation.

The conclusions reached in this study provide independent constraints on the environmental conditions at two well-known sites documenting important periods in the evolution of early amphibians. The Red Hill roadcut preserves some of the earliest amphibians and the Joggins Formation is home to the earliest known reptile. The analysis of phosphatic material from the Joggins Formation and the Red Hill roadcut exposure provide insight into the environmental conditions occurring alongside what is arguably the most important evolutionary adaptation, the evolution of terrestrial vertebrates. Understanding the environmental constraints that shaped the evolution of early

amphibians and reptiles can provide crucial insights into the factors that contribute to the decline of modern amphibian populations. By recognizing the importance of understanding and preserving habitats, we can take steps to ensure the survival of modern amphibians and other species in the face of ongoing environmental changes.

Table 1: $\delta^{18}O$ data collected from analyses on the Red Hill Roadcut. All $\delta^{18}O$ values are reported in parts per million (‰) relative to VSMOW.

Animal Species	Sample type sampled	Identifier 1	$\delta^{18}O$ Phosphate	Average $\delta^{18}O$ Phosphate	Average Calculated $\delta^{18}O_{water}$	Floodplain Habitat	$\delta^{18}O_{water}$ of floodplain habitat
Hynerpeton bassetti	Tooth (1)	1HT1	14.8	13.1	-4.8	Amphibious taxa	-3.9
		1HT3	12.9				
		1HT4	11.3				
		1HT5	13.0				
		1HT6	13.3				
Hynerpeton bassetti	Tooth (2)	2HT1	14.8	13.5	-4.4		
		2HT2	12.9				
		2HT5	13.1				
		2HT6	13.1				
Hynerpeton bassetti	Tooth (3)	3HT3	13.2	14.3	-3.6		
		3HT3	13.3				
		3HT5	15.6				
		3HT6	15.1				
Hynerpeton bassetti	Tooth (4)	4HT1	14.6	14.2	-3.7		
		4HT2	14.2				
		4HT3	14.5				
		4HT4	13.7				
Hynerpeton bassetti	Tooth (5)	5HT1	15.6	14.8	-3.1		
		5HT1 Dup.	15.5				
		5HT2	14.3				
		5HT3	14.5				
		5HT4	14.3				
Megalichthys mullisoni	Scale	BS1	14.0	13.4	-4.5		-4.5
		BS2	13.0				

Megalichthys mullisoni	Scale	BS3	13.6	13.4	-4.5	Either ponded waters or main channel	-4.5
		BS3 dup.	13.7				
		BS4	13.1				
		BS5	13.2				
Megalichthys mullisoni	Scale	SS1	13.4	14.0	-3.9		
		SS2	13.5				
		SS3	12.9				
		SS4	15.1				
		SS6	15.1				
Turrisaspis elektor	Dermal Plate Fragments	DPF	11.6	12.7	-5.2		
		DPF Dup.	11.4				
		DPF2	15.1				
		DPF3	12.7				
Rhizodontid	Partial Cleithurm	PCL3	12.7	13.7	-4.2	Ponded water	-3.6
		PCL4	14.1				
		PCL5	15.1				
		PCL6	12.8				
Gyracanthus sherwoodi	Partial fin spine	PFSL2	15.5	14.6	-3.2		
		PFSL5	15.1				
		PFSL8	13.3				
Gyracanthus sherwoodi	Partial fin spine	PFSS3	14.0	14.5	-3.4		
		PFSS4	14.8				
		PFSS5	14.8				
		PFSS6	14.2				
Hyneria lindae	Coronoid tooth	CT	13.7	14.7	-3.2	Main channel	-3.2
		CT1	16.0				
		CT1 Dup.	16.1				
		CT2	15.0				
		CT3	14.9				
	Jawbone	JBB1	14.5				

Hyneria lindae	Jawbone	JBB2	14.0	14.7	-3.2	Main channel	-3.2
		JBB4	14.0				
		JBB5	14.1				
		SJBL3	14.4				
		SJBL4	14.5				
		SJBL5	15.0				

Table 2: $\delta^{18}O$ data collected from analyses on the Joggins Formation. All $\delta^{18}O$ values are reported in parts per million (‰) relative to VSMOW.

Meters from the base	$\delta^{18}O_{phosphate}$	Average $\delta^{18}O_{phosphate}$ per stratigraphic unit	$\delta^{18}O$ water at T=20˚C	Average $\delta^{18}O_{water}$ T=20˚C	$\delta^{18}O$ water at T=25˚C	Average $\delta^{18}O_{water}$ T=25˚C	$\delta^{18}O$ water at T=30˚C	Average $\delta^{18}O_{water}$ T=30˚C
915.5	13.7	13.7	-7.9	-7.9	-6.8	-6.8	-5.7	-5.7
872	14.7	15.5	-6.9	-6.1	-5.8	-5.0	-4.7	-3.9
	14.8		-6.9		-5.8		-4.6	
	16.4		-5.2		-4.1		-3.0	
	16.1		-5.6		-4.5		-3.4	
820.3	12.8	13.2	-8.9	-8.4	-7.8	-7.3	-6.6	-6.2
	13.6		-8.0		-6.9		-5.8	
554	13.8	13.7	-7.9	-8.0	-6.8	-6.9	-5.6	-5.7
	13.6		-8.1		-7.0		-5.8	
547	13.3	14.1	-8.3	-7.6	-7.2	-6.5	-6.1	-5.4
	14.8		-6.9		-5.7		-4.6	
448.4	12.9	12.6	-8.7	-9.0	-7.6	-7.9	-6.5	-6.8

448.4	12.3		-9.4		-8.3		-7.1	
189	12.5	12.8	-9.1	-8.9	-8.0	-7.8	-6.9	-6.7
	13.3		-8.4		-7.2		-6.1	
	12.5		-9.1		-8.0		-6.9	
148.4	12.5	13.2	-9.2	-8.4	-8.1	-7.3	-7.0	-6.2
	13.9		-7.7		-6.6		-5.5	
148.2	12.4	13.1	-9.2	-8.5	-8.1	-7.4	-7.0	-6.3
	13.3		-8.3		-7.2		-6.1	
	13.2		-8.4		-7.3		-6.2	
	13.5		-8.1		-7.0		-5.9	
73.5	13.3	13.3	-8.3	-8.3	-7.2	-7.2	-6.1	-6.1
	13.3		-8.4		-7.3		-6.1	
35.5 – 15cm	13.4	13.5	-8.3	-8.2	-7.2	-7.1	-6.0	-6.0
	13.5		-8.1		-7.0		-5.9	
35.5	13.4	13.9	-8.3	-7.7	-7.2	-6.6	-6.0	-5.5

35.5	14.5		-7.2		-6.1		-4.9	

References

Algeo, T.J., and Scheckler, S.E., 1998, Terrestrial-marine teleconnections in the Devonian: links between the evolution of land plants, weathering processes, and marine anoxic events: Philosophical transactions of the Royal Society of London. Series B, Biological sciences, v. 353, p. 113–130, doi:10.1098/rstb.1998.0195.

Allaby, M., 2020, A dictionary of zoology A dictionary of zoology: London, England, Oxford University Press, doi:10.1093/acref/9780198845089.001.0001.

Berner, R.A., 2009, Phanerozoic atmospheric oxygen: New results using the GEOCARBSULF model: American Journal of Science, v. 309, p. 603–606, doi:10.2475/07.2009.03.

Blieck, A., Clement, G., Blom, H., Lelievre, H., Luksevics, E., Streel, M., Thorez, J., and Young, G.C., 2007, The biostratigraphical and palaeogeographical framework of the earliest diversification of tetrapods (Late Devonian): Geological Society special publication, v. 278, p. 219–235, doi:10.1144/sp278.10.

Brand, U., 1994, Continental hydrology and climatology of the Carboniferous Joggins Formation (lower Cumberland Group) at Joggins, Nova Scotia: evidence from the geochemistry of bivalves: Palaeogeography, Palaeoclimatology, Palaeoecology, v. 106, p. 307–321, doi:10.1016/0031-0182(94)90016-7.

Brand, U., Yochelson, E.L., and Eagar, R.M., 1993, Geochemistry of late Permian non-marine bivalves: Implications for the continental paleohydrology and paleoclimatology of northwestern China: Carbonates and Evaporites, v. 8, p. 199–212, doi:10.1007/bf03175178.

Breitburg, D., 2002, Effects of hypoxia, and the balance between hypoxia and enrichment, on coastal fishes and fisheries: Estuaries, v. 25, p. 767–781, doi:10.1007/bf02804904.

Calder, J.H., 1998, The Carboniferous evolution of Nova Scotia: Geological Society special publications, v. 143, p. 261–302, doi:10.1144/GSL.SP.1998.143.01.19.

Carpenter, D.K., Falcon-Lang, H.J., Benton, M.J., and Grey, M., 2015, Early Pennsylvanian (Langsettian) fish assemblages from the Joggins Formation, Canada, and their implications for palaeoecology and palaeogeography: Palaeontology, v. 58, p. 661–690, doi:10.1111/pala.12164.

Carroll, R.L., 1964, The earliest reptiles: The Journal of the Linnean Society, v. 45, p. 61–83, doi:10.1111/j.1096-3642.1964.tb00488.x.

Clack, J., 2002, Gaining ground: The origin and early evolution of tetrapods: Bloomington, MN, Indiana University Press.

Climate History of the Bashkirian - Moscovian Scotese.com, http://www.scotese.com/ldevclim.htm (accessed April 2023).

Climate History of the Late Devonian Scotese.com, http://www.scotese.com/climate.htm (accessed April 2023).

Cloutier, R., Clement, A.M., Lee, M.S.Y., Noël, R., Béchard, I., Roy, V., and Long, J.A., 2020, Author Correction: Elpistostege and the origin of the vertebrate hand: Nature, v. 583, p. E28, doi:10.1038/s41586-020-2450-2.

Comparing oxygen isotope records of Silurian calcite and phosphate- δ18O compositions of brachiopods and conodonts Geochimica et Cosmochimica Acta, v. 64, p. 1859–1872.

Conroy, J.L., Thompson, D.M., Cobb, K.M., Noone, D., Rea, S., and LeGrande, A.N., 2017, Spatiotemporal variability in the $\delta^{18}O$ -salinity relationship of seawater across the tropical Pacific Ocean: Isotope-Salinity Relationships: Paleoceanography, v. 32, p. 484–497, doi:10.1002/2016PA003073.

Cressler, W.L., 2006, Plant paleoecology of the Late Devonian Red Hill locality, north-central Pennsylvania, an *Archaeopteris*-dominated wetland plant community and early tetrapod site, *in* Wetlands through Time, Geological Society of America, p. 79- 102.

Cressler, W. L., Daeschler E. B., Slingerland, R., Peterson, D. A., 2010, Terrestrialization in the Late Devonian: A palaeoecological overview of the Red Hill site, Pennsylvania, USA: Gaël Clement and Marco Vecoli [eds.], The Terrestrialization Process: Modelling Complex Interactions at the Biosphere-Geosphere Interface, p. 111–128,

Crowson, R.A., Showers, W.J., Wright, E.K., and Hoering, T.C., 1991, Preparation of phosphate samples for oxygen isotope analysis: Analytical Chemistry, v. 63, p. 2397–2400, doi:10.1021/ac00020a038.

Daeschler, E.B., 2000, Early tetrapod jaws from the late Devonian of Pennsylvania, USA: Journal of Paleontology, v. 74, p. 301–308, doi:10.1666/0022-3360(2000)074<0301:etjftl>2.0.co;2.

Daeschler, E.B., Clack, J.A., and Shubin, N.H., 2009, Late Devonian tetrapod remains from Red Hill, Pennsylvania, USA: how much diversity? Acta Zoologica (Stockholm, Sweden), v. 90, p. 306–317, doi:10.1111/j.1463-6395.2008.00361.x.

Daeschler, E.B., and Cressler, W.L., III, 2011, Late Devonian paleontology and paleoenvironments at Red Hill and other fossil sites in the Catskill Formation of north-central Pennsylvania, *in* From the Shield to the Sea: Geological Field Trips from the 2011 Joint Meeting of the GSA Northeastern and North-Central Sections, Geological Society of America, p. 1–16.

Daeschler, E.B., Frumes, A.C., and Mullison, C.F., 2003, Groenlandaspidid placoderm fishes from the Late Devonian of North America: Records of the Australian Museum, v. 55, p. 45–60, doi:10.3853/j.0067-1975.55.2003.1374.

Daeschler, E.B., and Shubin, N., 1995, Tetrapod origins: Paleobiology, v. 21, p. 404–409, doi:10.1017/s0094837300013452.

Daeschler, E.B., Shubin, N.H., Thomson, K.S., and Amaral, W.W., 1994, A Devonian tetrapod from North America: Science (New York, N.Y.), v. 265, p. 639–642, doi:10.1126/science.265.5172.639.

Davies, S.J., Gibling, M.R., Rygel, M.C., Calder, J.H., and Skilliter, D.M., 2005, The Pennsylvanian Joggins Formation of Nova Scotia: sedimentological log and stratigraphic framework of the historic fossil cliffs: Atlantic geology, v. 41, doi:10.4138/182.

Dawson, J.W., 1882, On the results of recent explorations of erect trees containing animal remains in the coal formation of Nova Scotia; Philosophical Transactions of the Royal Society of London, v. 173, p. 621–659.

Dawson, J.W., 1896, Additional report on erect trees containing animal remains in the Coal Formation of Nova Scotia: Proceedings of the Royal Society of London, v. 59, p. 362–366.

Dolby , G., 1991, The palynology of the western Cumberland Basin, Nova Scotia: Nova Scotia Department of Natural Resources Open File Report 91–006, p. 39

Elger, A., Bornette, G., Barrat-Segretain, M.-H., and Amoros, C., 2004, Disturbances as a structuring factor of plant palatability in aquatic communities: Ecology, v. 85, p. 304–311, doi:10.1890/02-0752.

Falcon-Lang, H.J., 2003, Anatomically-preserved cordaitalean trees from Lower Pennsylvanian (Langsettian) dryland alluvial-plain deposits at Joggins, Nova Scotia: Atlantic geology, v. 39, doi:10.4138/1185.

Falcon-Lang, H.J., Benton, M.J., Braddy, S.J., and Davies, S.J., 2006, The Pennsylvanian tropical biome reconstructed from the Joggins Formation of Nova Scotia, Canada: Journal of the Geological Society, v. 163, p. 561–576, doi:10.1144/0016-764905-063.

Falcon-Lang, H.J., and Calder, J.H., 2004, Feature: UNESCO world heritage and the Joggins cliffs of Nova Scotia: Geology Today, v. 20, p. 139–143, doi:10.1111/j.1365-2451.2004.00469.x.

Falcon-Lang, H.J., Gibling, M.R., and Grey, M., 2010, Joggins, Nova Scotia: Geology Today, v. 26, p. 108–114, doi:10.1111/j.1365-2451.2010.00755.x.

Firsching, F.H., 1961, Precipitation of silver phosphate from homogenous solution: Analytical Chemistry, v. 33, p. 873–874, doi:10.1021/ac60175a018.

Fisheries, N., 2021, Age validation of pacific cod using stable oxygen isotope ($\delta^{18}O$) in otoliths: NOAA, https://www.fisheries.noaa.gov/feature-story/age-validation-pacific-cod-using-stable-oxygen-isotope-δ18o-otoliths (accessed April 2023).

Gat, J.R., 1996, Oxygen and hydrogen isotopes in the hydrologic cycle: Annual review of earth and planetary sciences, v. 24, p. 225–262, doi:10.1146/annurev.earth.24.1.225.

George, D., and Blieck, A., 2011, Rise of the earliest tetrapods: an early Devonian origin from marine environment: PloS one, v. 6, p. e22136, doi:10.1371/journal.pone.0022136.

Godfrey, S.J., Fiorillo, A.R., and Carroll, R.L., 1987, A newly discovered skull of the temnospondyl amphibian Dendrerpeton acadianum Owen: Canadian Journal of Earth Sciences, v. 24, p. 796–805, doi:10.1139/e87-077.

Grey, M., Pufahl, P.K., and Aziz, A.A., 2011, Using multiple environmental proxies to determine degree of marine influence and paleogeographical position of the Joggins fossil cliffs, UNESCO world heritage site: Palaios, v. 26, p. 256–263, doi:10.2110/palo.2010.p10-118r.

Grossman, E.L., and Joachimski, M.M., 2022, Ocean temperatures through the Phanerozoic reassessed: Scientific reports, v. 12, p. 8938, doi:10.1038/s41598-022-11493-1.

Guy, S.-V., Thomas, T., Irit, Z., Andreas, P., Dorit, S., Omri, L., Ayelet, G., and Guy, B.-O., 2018, Tooth oxygen isotopes reveal Late Bronze Age origin of Mediterranean fish aquaculture and trade: Scientific reports, v. 8, p. 14086, doi:10.1038/s41598-018-32468-1.

J.R. Gat, R. Gonfiantini, M. Magaritz, Y. Yurtsever, P. Fritz, C. Panich, J.Ch. Fontes, B.R. Payne, 1981, Stable isotope hydrology. Deuterium and oxygen-18 in the water cycle: International Atomic , v. 210, p. 103–298, doi:10.1016/0012-8252(83)90069-7.

Harland, W. B., Armstrong, R. L., Cox, A.V., Craig, L.E., Smith, A. G., Smith, D. G., 1990, A Geologic Time Scale: Cambridge University Press, v. 128, p. 289–290, doi:10.1017/s0016756800022172.

Lécuyer, C., 2004, Oxygen Isotope Analysis of Phosphate, *in* Handbook of Stable Isotope Analytical Techniques, Elsevier, p. 482–496.

Lécuyer, C., 2004, New insights into the non-destructive analysis of fossil bone and teeth using infrared spectroscopy: Journal of Archaeological Sciences , v. 31, 5 , p. 623-634

Lécuyer, C., Amiot, R., Touzeau, A., and Trotter, J., 2013, Calibration of the phosphate $\delta^{18}O$ thermometer with carbonate–water oxygen isotope fractionation equations: Chemical Geology, v. 347, p. 217–226, doi:10.1016/j.chemgeo.2013.03.008.

Lécuyer, C., Grandjean, P., O'Neil, J.R., Cappetta, H., and Martineau, F., 1993, Thermal excursions in the ocean at the Cretaceous—Tertiary boundary (northern Morocco): $\delta^{18}O$ record of phosphatic fish debris: Palaeogeography, Palaeoclimatology, Palaeoecology, v. 105, p. 235–243, doi:10.1016/0031-0182(93)90085-w.

Le Hir, G., Donnadieu, Y., Goddéris, Y., Meyer-Berthaud, B., Ramstein, G., and Blakey, R.C., 2011, The climate change caused by the land plant invasion in the Devonian: Earth and planetary science letters, v. 310, p. 203–212, doi:10.1016/j.epsl.2011.08.042.

Longinelli, A., and Nuti, S., 1973, Revised phosphate-water isotopic temperature scale: Earth and Planetary Science Letters, v. 19, p. 373–376, doi:10.1016/0012-821x(73)90088-5.

McGhee, G.R., Jr, Orth, C.J., Quintana, L.R., Gilmore, J.S., and Olsen, E.J., 1986, Late Devonian "Kellwasser Event" mass-extinction horizon in Germany: No geochemical evidence for a large-body impact: Geology, v. 14, p. 776, doi:10.1130/0091-7613(1986)14<776:ldkemh>2.0.co;2.

McNamara. K, S.S., 1993, Strangers on the shore: New Scientist , p. 23–27.

Monjerezi, M., Vogt, R.D., Aagaard, P., Gebru, A.G., and Saka, J.D.K., 2011, Using 87Sr/86Sr, $\delta^{18}O$ and δ2H isotopes along with major chemical composition to assess groundwater salinization in lower Shire valley, Malawi: Applied Geochemistry: Journal of the International Association of Geochemistry and Cosmochemistry, v. 26, p. 2201–2214, doi:10.1016/j.apgeochem.2011.08.003.

Newham, E. et al., 2020, Reptile-like physiology in Early Jurassic stem-mammals: Nature Communications, v. 11, p. 5121, doi:10.1038/s41467-020-18898-4.

O'Neil, J.R., Roe, L., Reinhard, E., Blake, R.E., 1994, A rapid and precise method of oxygen isotopeanalysis of biogenic phosphate: Israel Journal of Earth Science , v. 43, p. 203–212.

Peterson, A.D., 2010, Stratigraphy and Paleoenvironments of the Red Hill site near Hyner, Pennsylvania: The Pennsylvania State University, https://etda.libraries.psu.edu/files/final_submissions/1312.

Pucéat, E. et al., 2010, Revised phosphate–water fractionation equation reassessing paleotemperatures derived from biogenic apatite: Earth and Planetary Science Letters, v. 298, p. 135–142, doi:10.1016/j.epsl.2010.07.034.

Rasch, L.J., Martin, K.J., Cooper, R.L., Metscher, B.D., Underwood, C.J., and Fraser, G.J., 2016, An ancient dental gene set governs development and continuous regeneration of teeth in sharks: Developmental Biology, v. 415, p. 347–370, doi:10.1016/j.ydbio.2016.01.038.

Retallack, G.J., 2011, Woodland hypothesis for Devonian tetrapod evolution: The Journal of Geology, v. 119, p. 235–258, doi:10.1086/659144.

Ricci, J., Quidelleur, X., Pavlov, V., Orlov, S., Shatsillo, A., and Courtillot, V., 2013, New 40Ar/39Ar and K–Ar ages of the Viluy traps (Eastern Siberia): Further evidence for a relationship with the Frasnian–Famennian mass extinction: Paleogeography, palaeoclimatology, paleoecology, v. 386, p. 531–540, doi:10.1016/j.palaeo.2013.06.020.

Romer, A.S., 1958, Tetrapod limbs and early tetrapod life: Evolution; International Journal Of Organic Evolution, v. 12, p. 365–369, doi:10.1111/j.1558-5646.1958.tb02966.x.

Rosenau, N.A., Tabor, N.J., Elrick, S.D., and Nelson, W.J., 2013, Polygenetic history of paleosols in middle-upper Pennsylvanian cyclothems of the Illinois basin, U.S.A.: Part II. Integrating geomorphology, climate, and glacioeustasy: Journal of Sedimentary Research, v. 83, p. 637–668, doi:10.2110/jsr.2013.51.

Ryan, R.J., Boehner, R.C., Calder, J.H., 1991, Lithostratigraphic Revisions of the upper Carboniferous to lower Permian strata in the Cumberland Basin, Nova Scotia and the regional implications for the Maritimes Basin in Atlantic Canada: Bulletin of Canadian Petroleum Geology, v. 39, p. 289–314.

Saline water and salinity Usgs.gov, https://www.usgs.gov/special-topics/water-science-school/science/saline-water-and-salinity (accessed April 2023).

Scheckler, S.E., 1978, Ontogeny of progymnosperms. II. Shoots of upper Devonian archaeopteridales: Canadian journal of botany. Journal Canadien De Botanique, v. 56, p. 3136–3170, doi:10.1139/b78-376.

Schoeninger, M.J., and DeNiro, M.J., 1982, Carbon isotope ratios of apatite from fossil bone cannot be used to reconstruct diets of animals: Nature, v. 297, p. 577–578, doi:10.1038/297577a0.

Scotese, C.R., Song, H., Mills, B.J.W., and van der Meer, D.G., 2021, Phanerozoic paleotemperatures: The earth's changing climate during the last 540 million years: Earth-Science Reviews, v. 215, p. 103503, doi:10.1016/j.earscirev.2021.103503.

Scotese, C.R., 2014, Atlas of Permo-Carboniferous Paleogeographic Maps (Mollweide Projection), Maps 53 – 64, Volumes 4, The Late Paleozoic, PALEOMAP Atlas for ArcGIS, PALEOMAP Project, Evanston, IL.

Sharp, Z., 2017, Principles of Stable Isotope Geochemistry, Second edition:, doi:10.25844/h9q1-0p82.

Shubin, N.H., Daeschler, E.B., and Jenkins, F.A., Jr, 2006, The pectoral fin of *Tiktaalik roseae* and the origin of the tetrapod limb: Nature, v. 440, p. 764–771, doi:10.1038/nature04637.

Simões, T.R., and Pierce, S.E., 2021, Sustained high rates of morphological evolution during the rise of tetrapods: Nature Ecology & Evolution, v. 5, p. 1403–1414, doi:10.1038/s41559-021-01532-x.

Stimson, M., Lucas, S., Melanson, G., 2012, The Smallest Known Tetrapod Footprints: Batrachichnus salamandroides from the Carboniferous of Joggins: Ichnos, v. 19, p. 127–140.

Sparkleen; 04-320-4, 04-320-5, S70110; Fisher Scientific; One Reagent Lane, Fair Lawn, NJ 07410; 11/21/2014

Streel, M., 2000, Late Frasnian–Famennian climates based on palynomorph analyses and the question of the Late Devonian glaciations: Earth-Science Reviews, v. 52, p. 121–173, doi:10.1016/s0012-8252(00)00026-x.

Sullivan, S.M., Watzin, S.M., 2009, Stream-floodplain connectivity and fish assemblage diversity in the Champlain Valley, Vermont, U.S.A: Journal of Fish Biology, v. 74, p. 1394–1418.

Thomson, K. S. 1968. A new Devonian fish (Crossopterygii: Rhipidistia) considered in relation to the origin of the Amphibia. Postilla 124:1–13.

Tibert, N.E., and Dewey, C.P., 2006, *Velatomorpha*, a new healdioidean ostracode genus from the early Pennsylvanian Joggins Formation, Nova Scotia, Canada: Micropaleontology, v. 52, p. 51–66, doi:10.2113/gsmicropal.52.1.51.

Traverse, A., 2003, Dating the earliest tetrapods: A catskill palynological problem in Pennsylvania: CFS Courier Forschungsinstitut Senckenberg, p. 19–29.

Trego, C., 2014, Paleoecological Analysis of a Late Devonian Catskill Formation: Lycoming College.

Tudge, A.P., 1960, A method of analysis of oxygen isotopes in orthophosphate and its use in measurements of paleotemperatures: Geochimica et Cosmoshimica Acta, v. 18, p. 81–93.

Turner, R.L., and Meyer, C.E., 1980, Salinity Tolerance of the Brackish-Water Echinoderm Ophiophragmus filograneus (Ophiuroidea): Marine Ecology Progress Series, v. 2, p. 249–256, doi:10.3354/meps002249.

Waldron, J.W.F., and Rygel, M.C., 2005, Role of evaporite withdrawal in the preservation of a unique coal-bearing succession: Pennsylvanian Joggins Formation, Nova Scotia: Geology, v. 33, p. 337, doi:10.1130/g21302.1.

Wang, Y., Wang, X., Xu, Y., Zhang, C., Li, Q., Tseng, Z.J., Takeuchi, G., and Deng, T., 2008, Stable isotopes in fossil mammals, fish and shells from Kunlun Pass Basin, Tibetan Plateau: Paleo-climatic and paleo-elevation implications: Earth and Planetary Science Letters, v. 270, p. 73–85, doi:10.1016/j.epsl.2008.03.006.

Woodrow, D.L., Fletcher, F.W., and Ahrnsbrak, W.F., 1973, Paleogeography and paleoclimate at the deposition sites of the Devonian Catskill and old red facies: Geological Society of America bulletin, v. 84, p. 3051, doi:10.1130/0016-7606(1973)84<3051:papatd>2.0.co;2.